

UNCLASSIFIED

SECURITY CLASSIFICATION OF THIS PAGE

REPORT DOCUMENTATION PAGE

1a. REPORT SECURITY CLASSIFICATION UNCLASSIFIED			1b. RESTRICTIVE MARKINGS			
2a. SECURITY CLASSIFICATION AUTHORITY			3. DISTRIBUTION / AVAILABILITY OF REPORT Approved for public release; distribution is unlimited			
2b. DECLASSIFICATION / DOWNGRADING SCHEDULE						
4. PERFORMING ORGANIZATION REPORT NUMBER(S) TR 87-01			5. MONITORING ORGANIZATION REPORT NUMBER(S)			
6a. NAME OF PERFORMING ORGANIZATION Naval Environmental Prediction Research Facility		6b. OFFICE SYMBOL (If applicable)		7a. NAME OF MONITORING ORGANIZATION		
6c. ADDRESS (City, State, and ZIP Code) Monterey, CA 93943-5006			7b. ADDRESS (City, State, and ZIP Code)			
8a. NAME OF FUNDING / SPONSORING ORGANIZATION Office of Naval Technology		8b. OFFICE SYMBOL (If applicable) Code 22		9. PROCUREMENT INSTRUMENT IDENTIFICATION NUMBER		
8c. ADDRESS (City, State, and ZIP Code) 800 N. Quincy St. Arlington, VA 22217			10. SOURCE OF FUNDING NUMBERS			
			PROGRAM ELEMENT NO. 62435N	PROJECT NO. 3582	TASK NO.	WORK UNIT ACCESSION NO. DN656769
11. TITLE (Include Security Classification) Meteorological Radar and its Usage in the Navy (U)						
12. PERSONAL AUTHOR(S) Hembree, Dr. Louis A., Jr.						
13a. TYPE OF REPORT Final		13b. TIME COVERED FROM 1/86 TO 3/87		14. DATE OF REPORT (Year, Month, Day) 1987, July		15. PAGE COUNT 67
16. SUPPLEMENTARY NOTATION						
17. COSATI CODES			18. SUBJECT TERMS (Continue on reverse if necessary and identify by block number) Remote sensing Environmental support Battle group Radar			
FIELD	GROUP	SUB-GROUP				
04	02					
17	09					
19. ABSTRACT (Continue on reverse if necessary and identify by block number) The basic principles of radar meteorology are presented along with the current capabilities of meteorological radars. Factors that need to be examined when evaluating a radar for meteorological applications are also discussed. The current use of radars for meteorological measurements within the Navy is presented along with possible future applications. It is concluded that Doppler meteorological radar data could have a significant impact on Naval operations. It is recommended that the replacement for the FPS-106 have Doppler capability with at least intensity and velocity displays. It is further recommended that the radar have the capacity to apply various application algorithms to the data. The ability to process weather information should be added to suitable afloat tactical radars.						
20. DISTRIBUTION / AVAILABILITY OF ABSTRACT <input checked="" type="checkbox"/> UNCLASSIFIED/UNLIMITED <input type="checkbox"/> SAME AS RPT. <input type="checkbox"/> DTIC USERS				21. ABSTRACT SECURITY CLASSIFICATION UNCLASSIFIED		
22a. NAME OF RESPONSIBLE INDIVIDUAL Dr. Louis A. Hembree, Jr.			22b. TELEPHONE (Include Area Code) (408) 647-4787		22c. OFFICE SYMBOL NEPRF WU 6.2-35	

AN (1) AD-A186 650
FG (2) 170900
FG (2) 040200
CI (3) (U)
CA (5) NAVAL ENVIRONMENTAL PREDICTION RESEARCH FACILITY
MONTEREY CA
TI (6) Meteorological Radar and its Usage in the Navy.
TC (8) (U)
DN (9) Final rept. Jan 86-Mar 87.
AU (10) Hembree, Louis A., Jr
RD (11) Jul 1987
PG (12) 67
RS (14) TR-87-01
PJ (16) 3582
RC (20) Unclassified report
ND (21) Original contains color plates: All DTIC and NTIS
reproductions will be in black and white.
DE (23) *DOPPLER SYSTEMS, *METEOROLOGICAL RADAR, *WEATHER,
ALGORITHMS, DISPLAY SYSTEMS, IMPACT, NAVAL OPERATIONS,
RADAR, TACTICAL WARFARE, VELOCITY.
DC (24) (U)
ID (25) PE62435N, WUDN656769.
IC (26) (U)
AB (27) The basic principles of radar meteorology are presented
along with the current capabilities of meteorological
radars. Factors that need to be examined when
evaluating a radar for meteorological applications are
also discussed. The current use of radars for
meteorological measurements within the Navy is
presented along with possible future applications. It
is concluded that Doppler meteorological radar data
could have significant impact on Naval operations. It
is recommended that the replacement for the FPS-106
have Doppler capability with at least intensity and
velocity displays. It is further recommended that the
radar have the capacity to apply various application
algorithms to the data. The ability to process weather
information should be added to suitable afloat tactical
radars.
AC (28) (U)
DL (33) 01
SE (34) F
CC (35) 407279

Naval Environmental Prediction Research Facility
Monterey, CA 93943-5006



Technical Report TR-87-01 July 1987

LIBRARY
RESEARCH REPORTS DIVISION
NAVAL POSTGRADUATE SCHOOL
MONTEREY, CALIFORNIA 93940

METEOROLOGICAL RADAR AND ITS USAGE IN THE NAVY.

Dr. Louis A. Hembree, Jr.

Naval Environmental Prediction Research Facility

QUALIFIED REQUESTORS MAY OBTAIN ADDITIONAL COPIES
FROM THE DEFENSE TECHNICAL INFORMATION CENTER.
ALL OTHERS SHOULD APPLY TO THE NATIONAL TECHNICAL
INFORMATION SERVICE.

CONTENTS

1.	Introduction	1
2.	Radar Meteorology	2
2.1	Intensity Considerations	3
2.1.1	Precipitation Estimation	7
2.2	Doppler Considerations	12
3.	Criteria for Radar Suitability Evaluation	17
3.1	Beam Width	17
3.2	Pulse Length/Range Resolution	23
3.3	Transmitted Power	23
3.4	Frequency	24
3.5	Polarization	25
4.	Current Capabilities	25
4.1	Intensity Data	25
4.2	Velocity	30
4.3	Returns in Optically Clear Air	40
5.	Current Meteorological Radar Status in the Navy	43
6.	Implementation of Radar Meteorology in the Navy	45
6.1	Ashore Installations	45
6.2	Afloat Installations	47
6.2.1	New Radar	50
6.2.2	Existing Tactical Radar	52
7.	Summary and Recommendations	56
	References	58
	Distribution	60

1. INTRODUCTION

The environment significantly affects the operation of the Navy, from the safety and performance of personnel and material to the planning of tactical operations. Meteorological radar is one method of remotely sensing the atmospheric environment. Historically, meteorological radars were limited to determining the position of storms and estimating the precipitation rate and storm intensity. Over the past decade or so with the development of digital processing, color displays, and Doppler meteorological radar, the amount of information that can be extracted and presented has greatly increased. This has resulted in increased utility of meteorological radar information.

This report has three main objectives: (a) to outline radar meteorology principles, (b) to report on the current applications of meteorological radars in the Navy, and (c) to present and discuss possible future applications of meteorological radars in the Navy.

Section 2 of this report contains a presentation of basic meteorological radar principles and the differences between Doppler and non-Doppler radars. Although this section provides a better framework for understanding meteorological radar usage and applications, it is not an essential requirement for understanding meteorological radar applications. Readers familiar with meteorological radar, or not desiring to read this background material, should skip Section 2. In Section 3, criteria for evaluating the applicability of a radar for meteorological applications are discussed. Section 4 presents the applications of conventional and Doppler meteorological radars. Section 5 discusses the current utilization of radars for meteorological applications in the Navy, both ashore and afloat. Section 6 discusses possible future use of meteorological radars in the Navy. Section 7 summarizes the conclusions of the report, and closes with a series of recommendations.

2. RADAR METEOROLOGY

This section contains a brief discussion of radar meteorology to introduce the reader to concepts and terminology used in radar meteorology. The discussion is restricted to pulsed radars. For further information, the reader is referred to Radar Observation of the Atmosphere by Louis J. Battan and Doppler Radar and Weather Observations by Richard J. Doviak and Dusan S. Zrnic'.

Meteorological radars are active devices; that is, they send out directional pulses of electromagnetic energy and measure the energy reflected by various targets. They typically operate in the frequency band between 3 and 30 GHz. This corresponds to wavelengths between 1 and 10 cm. A 10 cm wavelength is preferred because it is attenuated less by intervening precipitation and atmospheric gases. The shortest wavelength that is normally used for routine meteorological observations is 5 cm. Shorter wavelengths are used mainly for research.

The basic principle of operation is that a pulse of energy of duration, τ , is emitted by the radar (Figure 1). A portion of the transmitted energy is reflected by targets that are within

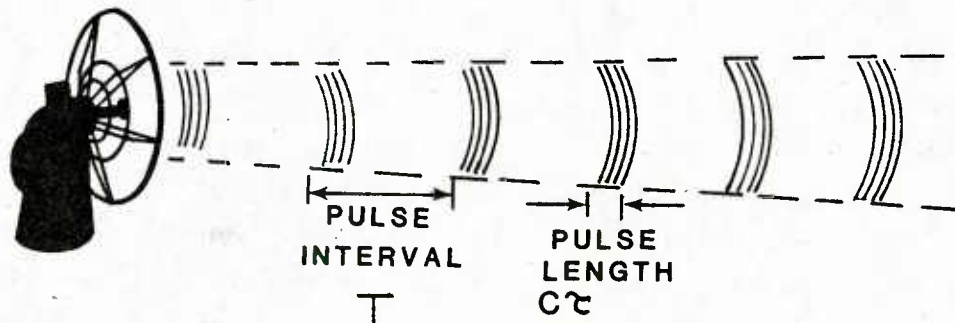


Figure 1. Representation of a pulse radar beam.

the beam. During the interval between pulses, the returned signal is detected and its strength measured. As will be shown later, the strength of the return can be related to the precipitation intensity. The distance to the target is determined by the elapsed time between the transmission of the pulse and the reception of the returned signal and is given by

$$r=ct/2, \quad (1)$$

where r is the range, c is the speed of light, and t is the elapsed time. The radar emits the pulses at a rate called the pulse repetition frequency, PRF. The pulse repetition period or pulse interval, T , is the reciprocal of the PRF. There exists a range beyond which the returned signal has not reached the radar before the next pulse has been emitted. This range is known as the maximum unambiguous range and is given by

$$r_{\max} = cT/2. \quad (2)$$

If there is a target at a range greater than r_{\max} , then its return for the n th pulse will be received after the $n+1$ pulse has been transmitted (Figure 2). Therefore, the elapsed time will appear to be $t' = t-T$ and the apparent range will be $r' = ct'/2 = ct/2 - r_{\max}$. Since the target will appear to be at a nearer range than it really is, the range is observed as ambiguous. To eliminate range ambiguities, all targets must lie within r_{\max} . Figure 3 is a plot of unambiguous range as a function of PRF.

2.1 Intensity Considerations

The power returned from the target is given by the radar equation. For a discrete target the radar equation is

$$\bar{P}_r = \frac{P_t G^2 \lambda^2 L^2 f^4(\theta, \phi) \sigma}{(4\pi)^3 r^4} \quad (3)$$

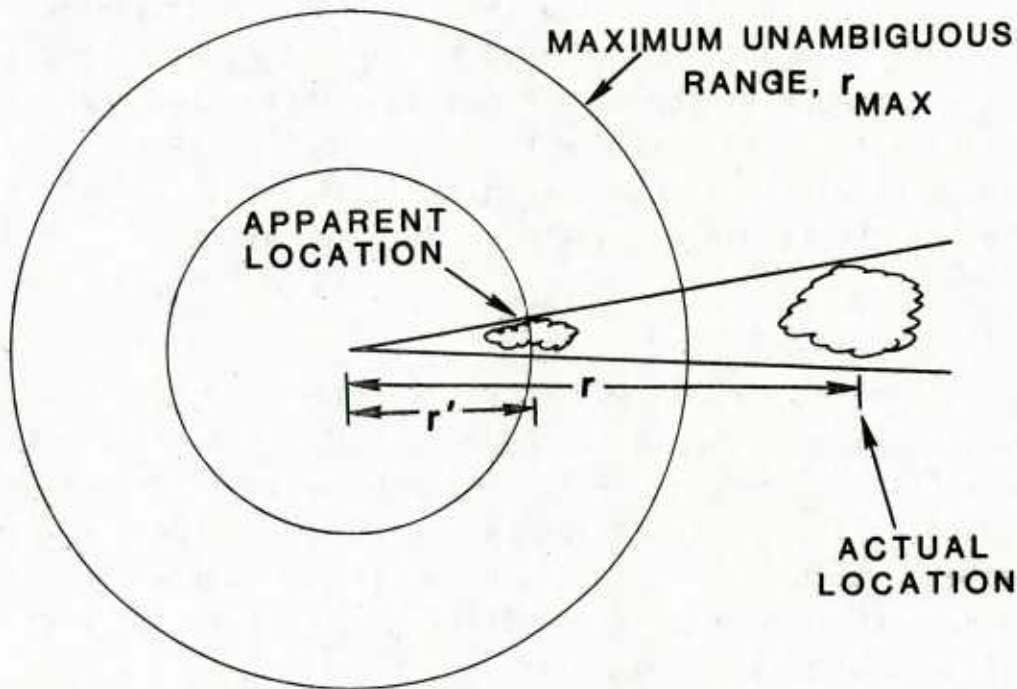


Figure 2. Example of a second trip echo. If target is at a range r , greater than the maximum unambiguous range r_{\max} , the target appears to be at range $r' = r - r_{\max}$.

where \bar{P}_r is the power received, P_t is the transmitted power, G is the antenna gain, L is the one way loss, σ is the backscatter cross section, λ is the wavelength, $f(\theta, \phi)$ is the antenna pattern function, and r is the range. In meteorology, however, we are not concerned with a single discrete target, but a distributed target comprised of many discrete targets contained in a single sample volume defined by the pulse length and beam width. If we assume a pencil beam with a half power beam width of θ and a Gaussian beam pattern in the main lobe, a pulse length of $h = ct/2$, and sum over the enclosed volume, we have

$$\bar{P}_r = \frac{P_t G^2 \lambda^2 L^2 h}{1024 \ln^2 \pi^2 r} \sum \sigma_i, \quad (4)$$

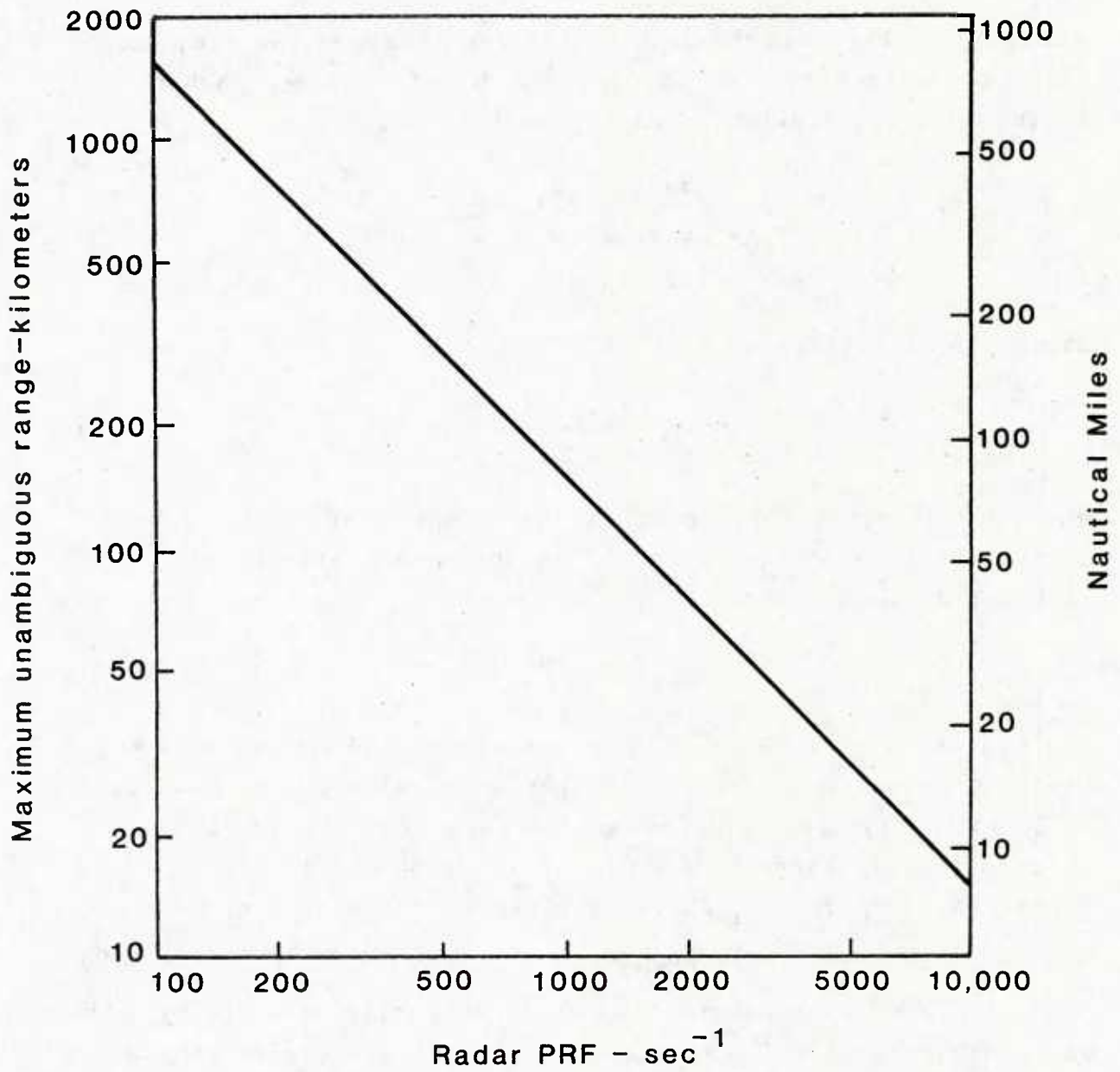


Figure 3. Maximum unambiguous range as a function of the pulse repetition frequency (PRF).

where the summation is over the sample volume. It can be shown that for Rayleigh scattering the backscatter cross section of a water drop is given by

$$\sigma_i = \frac{\pi^5 K^2}{\lambda^4} D_i^6, \quad (5)$$

where D_i is the diameter of the i th drop and K is the complex index of refraction. K^2 is equal to 0.93 for water. Substituting into the previous equation we get

$$P_r = \frac{\pi^3 P_t G^2 L^2 \theta^2 h}{1024 \ln 2 \lambda^2} \frac{K^2}{r^2} \sum D_i^6, \quad (6)$$

which can be rewritten as

$$P_r = \frac{C K^2}{r^2} Z_e, \quad (7)$$

where C is the radar constant which is dependent on the characteristics of the radar. Z is the radar reflectivity factor and is equal to

$$Z = \sum D_i^6, \quad (8)$$

and has units of mm^6/m^3 . Z is a measure of the strength of the target backscattering efficiency per unit volume. The magnitude of Z can easily range over several orders of magnitude for meteorological observations. For this reason it is often expressed in dB as dBZ, which is given by the equation

$$\text{dBZ} = 10 \text{ Log } Z. \quad (9)$$

Displays of meteorological radar intensity data are typically contours of dBZ. Typical modern radar receivers can detect signals as small as 10^{-14} Watts. The results of sample calculations of minimum detectable reflectivity factor at 25 nm range are presented in Table 1. Case 1 is for a radar that approximates

Table 1. Sample calculations using the meteorological radar equation for three hypothetical radars.

	CASE 1	CASE 2	CASE 3
Transmitted Power (MW)	1	1	1
Gain (dB)	46	39	39
Beam Width (Deg)	0.8	1.7	1.7
Pulse Length (m)	150	250	250
Wavelength (m)	0.1	0.1	0.1
Range (NM)	25	25	25
Minimum Detectable Signal (dBm)	-110	-110	-114
Reflectivity Factor (dBZ)	-11.4	-6.1	-10.1

Next Generation Weather Radar (NEXRAD) requirements. Cases 2 and 3 approximate afloat radars with two different assumed minimum detectable signals and assumed design characteristics.

2.1.1 Precipitation Estimation

It is often desired to estimate the precipitation rate using radar because of its large areal coverage and its high update rate. The intensity of the return can be related to the precipitation rate if the drop size distribution of the precipitation is known, and if it can be assumed to be uniform over the pulse volume. The next two sections present two methods for estimating the rain fall rate. One, the ZR relationship, has been used for many years. The other method, dual polarization, is still experimental, but appears to offer an improvement over the ZR relationship approach.

2.1.1.1 ZR Relationships

As stated, the precipitation rate can be related to the measured reflectivity factor if the drop size distribution is known. As drops size distributions are difficult to measure, however, empirical ZR relationships have been determined. The empirical expression used by most investigators is of the form

$$Z = AR^b, \quad (10)$$

where R is the rain rate in mm/hr and the reflectivity factor Z is in mm^6/m^3 . A and b are empirically determined constants. Many expressions have been developed over the years. Two of the most commonly used equations are:

$$\text{Stratiform rain: } Z = 200R^{1.6} \quad (11a)$$

(Marshall and Palmer, 1948),

$$\text{Thunderstorm rain: } Z = 486R^{1.37} \quad (11b)$$

(Jones, 1956).

Figure 4 is a plot of these relationships. Rain rate estimates should be made at wavelengths greater than or equal to 5 cm (6 GHz) as the attenuation at shorter wavelengths can cause serious error. The National Weather Service defines six precipitation intensities. Table 2 gives the dBZ ranges corresponding to each of the intensities.

Studies and experience have shown that rain rates estimated by radar and those measured using rain gages often differ by a factor of 2 or more. Some of the variation is due to sampling problems and matching the gage to the corresponding radar bin. Richards and Crozier (1981), however, showed that different drop size distributions giving the same Z could cause rainfall rates to differ by as much as a factor of 4. They also stated that the variability can be reduced by choosing the ZR relationship to be used based on the precipitation type. Further reduction in variability can be gained by integrating over space and time. Even after considering the uncertainty, the rain rate estimates still provide usable information. Rain gauges have also been used to 'calibrate' the radar estimates (Brandes, 1975; Crawford, 1977; Hembree and Eddy, 1979). As part of the NEXRAD program, the National Weather Service is attempting to use gauges to correct the radar rain estimates.

2.1.1.2 Dual Polarization

Seliga et al. (1982) show that improved estimates of the rain rate can be obtained using dual polarization methods. As mentioned previously, the estimation of rain rate is highly

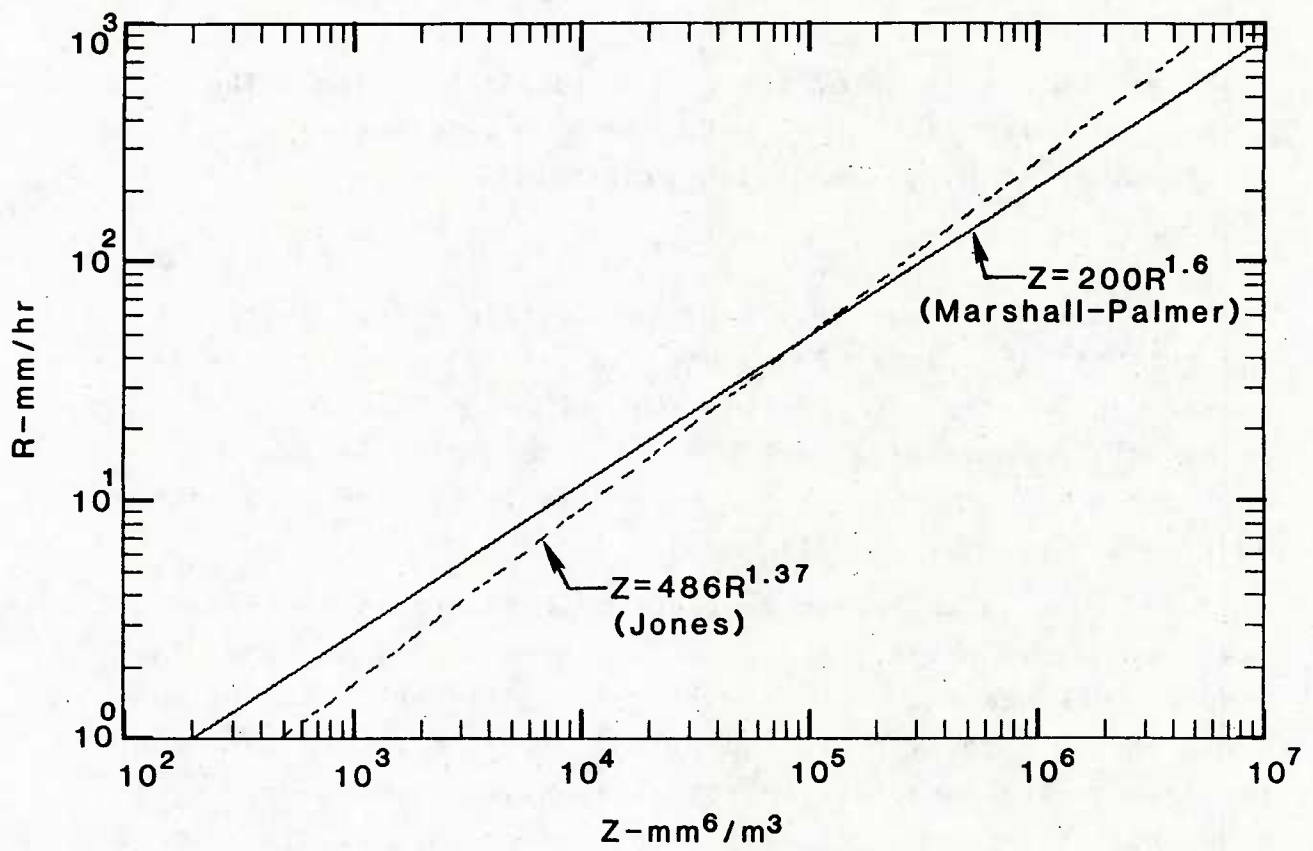


Figure 4. Plot of two commonly used ZR relationships.

Table 2. National Weather Service rain rate levels.

Level	Rainfall Category	Rainfall Rate (in/hr)	dBZ
1	light	< 0.1	< 30
2	moderate	0.1-0.5	30-41
3	heavy	0.5-1.0	41-46
4	very heavy	1.0-2.0	46-50
5	intense	2.0-5.0	50-57
6	extreme	> 5.0	> 57

dependent on knowledge of the drop size distribution. The distribution is usually assumed to be a two parameter distribution such as a negative exponential, ie.,

$$N(D) = N_0 \exp(-\Lambda D), \quad (12)$$

where N_0 and Λ are parameters of the distribution. When just the reflectivity factor Z was used to estimate rain fall rate, we were in principle trying to choose a two parameter model using only one measured variable. In the dual polarization approach, there are two variables available leading to a better model fit and improved estimates.

The dual polarization approach is based on the observation that rain drops are not spherical but have an oblate spheroidal shape. This means that they will react differently to horizontally and vertically polarized waves. It is expected that the returns for the horizontally polarized waves would be stronger than the return for vertically polarized waves. It can also be shown that the ratio Z_H/Z_V is a direct measure of the parameter Λ , where Z_H and Z_V are the measured reflectivity factors for the horizontally and vertically polarized waves respectively. A term called the differential reflectivity is defined as

$$Z_{DR} = 10 \log(Z_H/Z_V). \quad (13)$$

The resulting equations for rain rate estimation are typically in one of the following forms,

$$R = aZ_H 10^{bZ_{DR}} \quad (\text{Exponential Drop Distribution}) \quad (14a)$$

or

$$R = aZ_H^b Z_{DR}. \quad (\text{Gamma Drop Distribution}) \quad (14b)$$

In a single polarization meteorological radar the polarization is normally horizontal, and therefore $Z_H = Z$.

Another advantage of dual polarization radar is its ability to distinguish between the liquid and ice phases of precipitation. Table 3 (Hall et al., 1980) shows the expected characteristics of Z and Z_{DR} at a 10 cm wavelength. Notice the difference in characteristics for rain and dry frozen precipitation.

Table 3. Expected characteristics of Z and Z_{DR} at 10-cm wave length for various hydrometeor types (from Hall et al., 1980).

Hydrometeor Type	Z	Z_{DR}	Comments
Rain	High	High	Includes large oblate drops
Drizzle, cloud, or fog	Low	Low	Small spherical drops of water and/or small ice particles
Dry snow flakes	Medium-low	Medium-low	Large horizontally oriented low-density aggregates
Sleet/wet snow	High	High	Large oblate horizontally oriented particles
Wet graupel	High	Negative	Large conical vertically oriented particles
Wet hail	High	Variable	Large particles; seldom spheres.
Dry hail or other high-density ice particles	Medium	Low	

Dual polarization approaches are still in the research stage but are approaching readiness for operational implementation. Work still needs to be done on defining the empirical rain rate estimation relations.

2.2 Doppler Considerations

Besides measuring the intensity of the return, the newer generation of meteorological radars include a Doppler capability which allows them to measure the radial velocity and spectral width of the targets. This additional information increases the utility of the meteorological radar.

The total distance traveled by a pulse from the radar to the target and back is $2r$. Measured in wavelengths of the transmitted frequency, it is $2r/\lambda$ or in radians, $4\pi r/\lambda$. If the wave emitted by the radar has a phase of p_0 , the phase at reception would then be

$$p = p_0 - 4\pi r/\lambda \quad (15)$$

The time rate of change of phase is then

$$\frac{dp}{dt} = \frac{-4\pi}{\lambda} \frac{dr}{dt} = \frac{-4\pi V}{\lambda} \quad (16)$$

The quantity dp/dt is the angular frequency, ω , and is equal to $2\pi f$. Substitution gives

$$f = -2V/\lambda \quad (17)$$

where f is the Doppler shift frequency, and V is the radial velocity of the target (also called the Doppler velocity). Note that only the radial component of the velocity is measured. For meteorological targets the Doppler shift frequency is always in the audio range. Because the Doppler shift is in the audio range, it represents a very small change in the carrier frequencies used and would be difficult to measure with a single pulse. Therefore, the phase shift is measured over the longer period of time from pulse to pulse rather than during the pulse period.

From sampling theory it is known that to measure a frequency f , samples must be taken at a frequency of at least $2f$. Since the sampling rate is set at the PRF, the maximum Doppler shift frequency is

$$f_{\max} = \text{PRF}/2 \quad (18)$$

which corresponds to a maximum Doppler velocity of

$$V = (\text{PRF})\lambda/2. \quad (19)$$

Velocities in the sample volume greater than V_{\max} fold into the range $\pm V_{\max}$. This is known as aliasing or velocity folding and is illustrated in Figure 5. Since the maximum unambiguous range r_{\max} is also a function of the PRF, we have

$$V_{\max} = \lambda c/8r_{\max}. \quad (20)$$

Therefore, r_{\max} , V_{\max} , and the PRF are all related. If you want to change one, the other two are affected. Figure 6 is a plot of the relationship between r_{\max} and V_{\max} for various wavelengths.

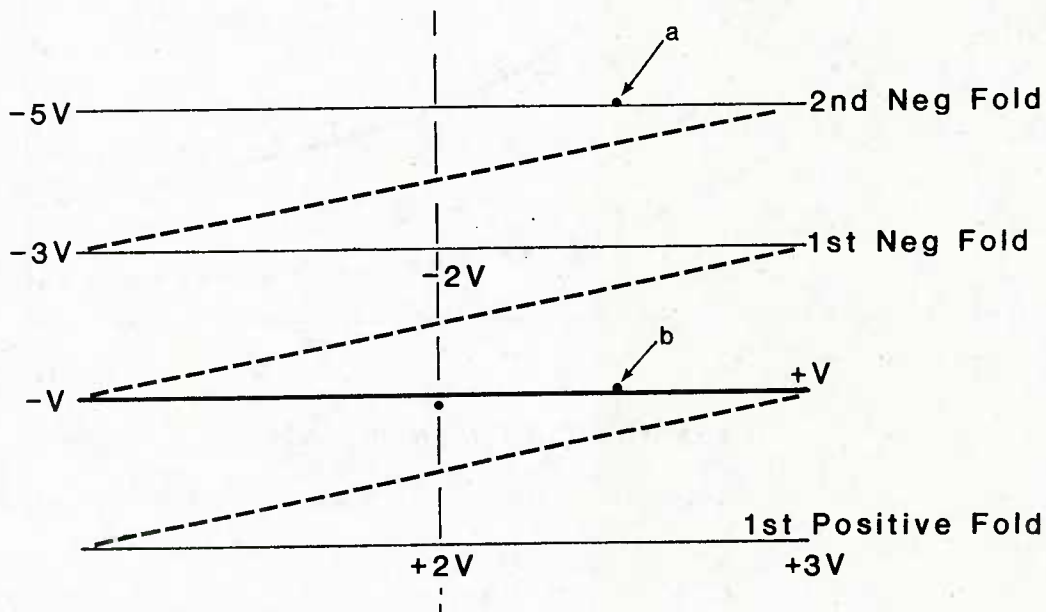


Figure 5. Illustration of aliasing. The unambiguous velocity is $\pm V$. Those velocities outside this range appear (fold into within this range). For example a real negative velocity of $-3.5V$ (point a) will appear as a velocity of $+0.5V$ (point b).

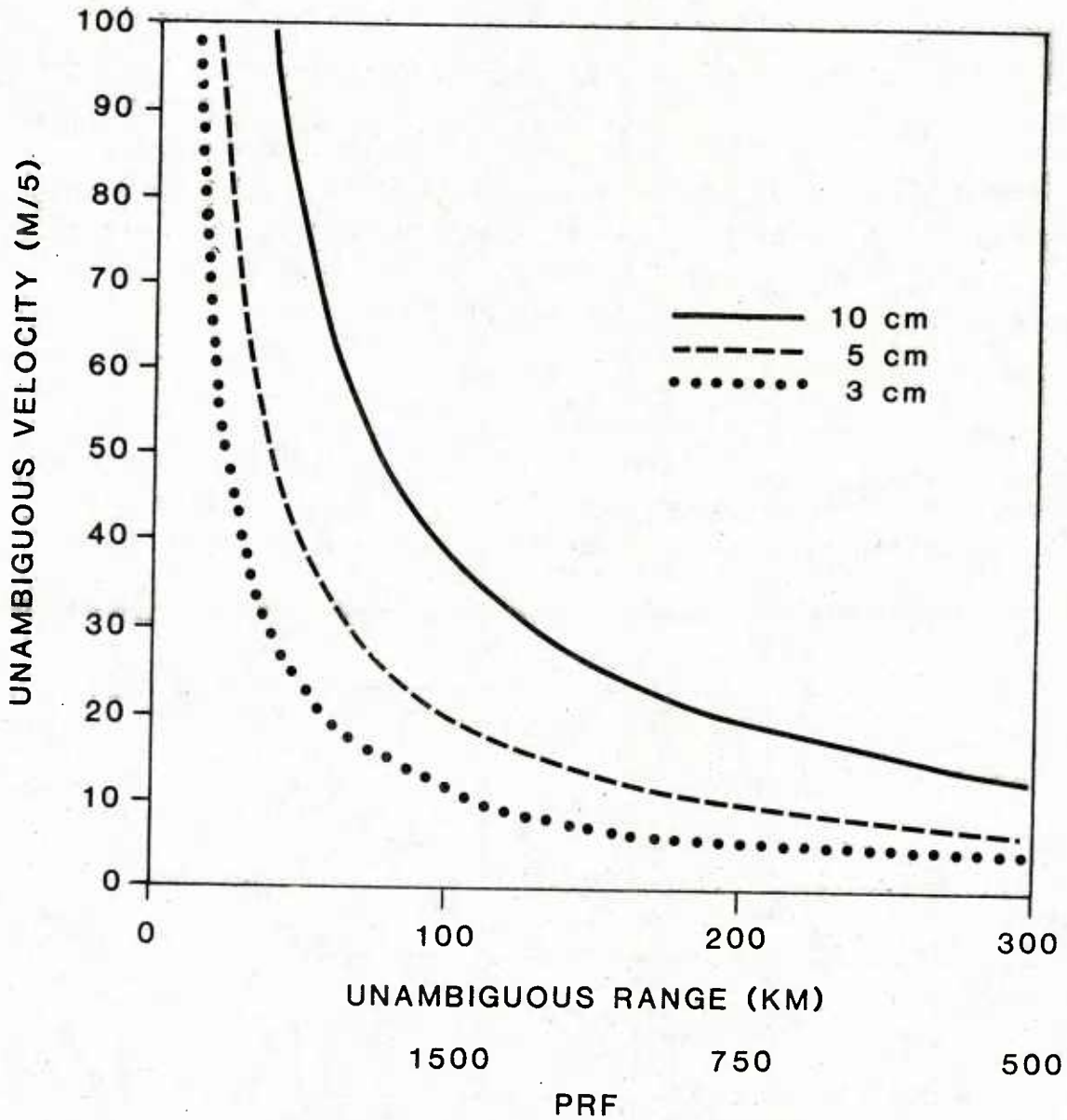


Figure 6. Plot of the relationship between unambiguous velocity and unambiguous range. The pulse repetition frequency (PRF) is also plotted along the X-axle. Notice that as the wavelength decreases, the unambiguous velocity also decreases for a given unambiguous range (PRF).

As discussed before, discrete volumes are being sampled. Each volume contains targets moving at many velocities (Figure 7). Therefore the phase shift measured at any one time is a weighted average of the phase shifts due to all of the targets in the sampling volume. The weighting is a function of location in the beam and the strength of their return. In general the stronger the return, and the closer to the beam center line, the larger the weighting. Because the resultant phase shift of a mean value varies, repeated samples are taken to obtain a statistically significant velocity estimate and to reduce the uncertainty in the estimate. This distribution is known as the velocity spectrum (Figure 8). The standard deviation of the spectrum is known as the spectrum variance or spectrum width and is a measure of the velocity dispersion.

Several factors can affect the magnitude of the observed spectrum width:

- (1) Systematic wind shear within the sample volume. This means that one portion of the beam will see a different velocity than another and the spectral width will be increased.
- (2) The spread of terminal velocities of the echoing targets. The larger the range of effective rain drop sizes, the larger is the spectrum variance. This effect is the greatest when the antenna is pointed vertically and is negligible when pointing horizontally.
- (3) The turbulence spectrum of the air. The smaller rain drops, ice particles, and dust respond faithfully to rapid changes in air motion and, therefore, reproduce the air velocities due to turbulence. Hence, the greater the turbulence, the larger the spectrum width.

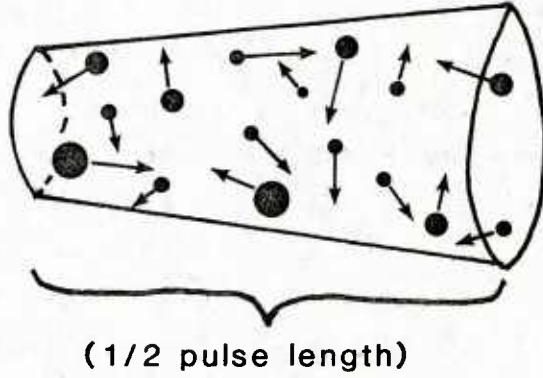


Figure 7. Target motion within an echo sample volume. The Doppler velocity measured is a weighted mean of the velocities contained in the sample volume. The larger the range of radial velocities in the sample volume, the greater the spectral width.

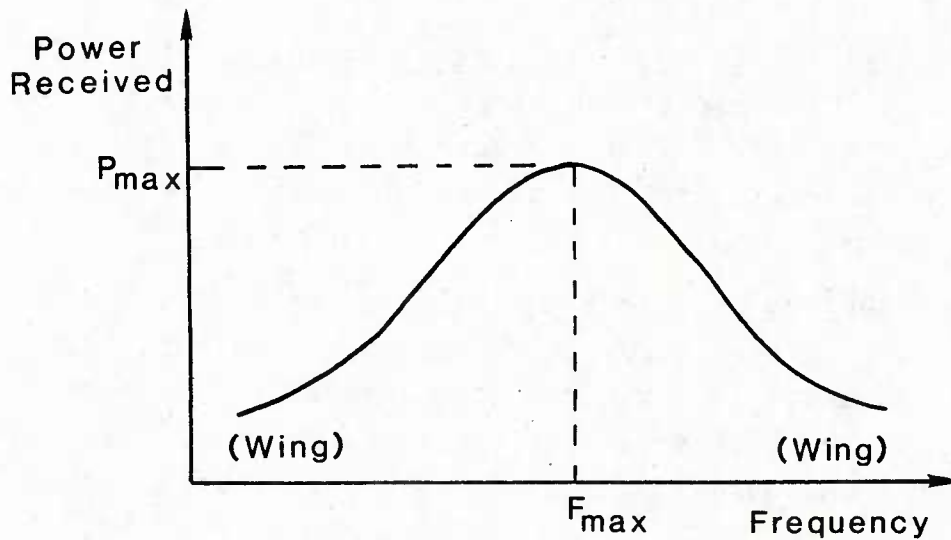


Figure 8. Idealized Doppler spectrum of a precipitation target. The X-axis frequency is the Doppler shift frequency and corresponds to radial velocity.

- (4) Finite beam width with uniform air motion across the radar beam. If the wind is perpendicular to the beam axis, then targets near the edge of the beam will produce a larger Doppler shift than those near the center where the Doppler shift would be zero (Figure 9).
- (5) Antenna motion. As the antenna rotates, the beam sweeps through space. Hence the radar does not receive echoes from identically weighted targets on successive samples which results in an increased spectrum width. The spectrum width increases as the antenna rotation rate increases.

3. CRITERIA FOR RADAR SUITABILITY EVALUATION

Several factors need to be considered when evaluating a radar for meteorological applications. Many are interrelated, and an improvement in one may result in a degradation in another. The relative merits of the factors must be weighed and a compromise reached. This section discusses these factors and tradeoffs.

3.1 Beam Width

Most meteorological radars have beam widths between 0.8 and 2.0°, with values near 1.0° preferred. There are four adverse effects associated with an increase in the beam width: 1) partial beam filling, 2) poorer rain rate measurement, 3) decreased spatial resolution, and 4) increased spectral width.

An assumption implicit in the derivation of the meteorological radar equation (Eq. 7) is that the beam is uniformly filled with scatterers. If the beam is not filled, the estimate of precipitation intensity is then in error. In Table 4 the diameters of the beam for different ranges and beam widths are given. At 25 nm, a 4° beam has a diameter over 3000 meters and partial beam filling will be a problem. If the beam width is doubled, the probability that the beam will not be filled is greatly increased.

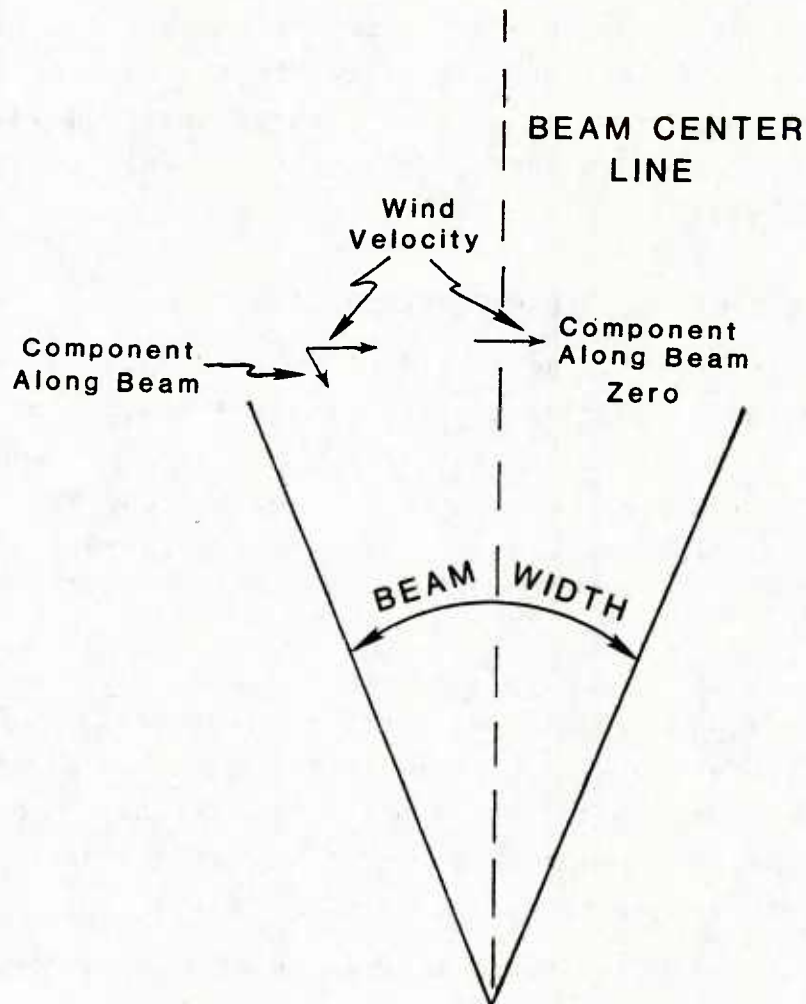


Figure 9. Example of spectrum broadening due to a uniform wind blowing across a beam of finite width. At the center line the radial component is zero. As the angle from the center line increases, the radial component also increases. This leads to a range of velocities being contained in the sample volume, hence an increased spectral width.

Table 4. Tabulation of beam diameters (meters) for various beam widths and ranges.

BEAM WIDTH (DEG)	RANGE (nm)		
	5	25	50
1.0	160	810	1620
1.5	240	1210	2420
4.0	650	3230	6460

Increased beam width has another effect on precipitation measurement other than that caused by incomplete beam filling. The range to which effective precipitation rates can be measured, even if the beam is filled, can be reduced as the beam width is increased. There is often a layer of enhanced returns, the bright band, caused by the melting snow as it falls through the melting layer (Figure 10). Within this layer the ZR relationships (Eq. 10) do not hold. Therefore, range cells that include the bright band cannot be used for rain rate estimation. Figure 11 illustrates this effect.

As the beam width increases, the transverse spatial resolution of the radar also decreases. With a decrease in resolution, significant features of precipitating regions will be smoothed. The smoothing could be sufficient to mask important features. Small intense rain or hail shafts could be smoothed to the extent that they could be missed.

Increasing the beam width also has an adverse affect on the Doppler velocity measurement. As the beam width increases the uncertainty of the velocity estimate is increased, as discussed in Section 2.2.

Using small beam widths can increase system costs. With a small beam width more data must be collected to cover the same area. This means that faster processing of the data is required. The cost and the size of the antenna system also increases. If the beam width is to be reduced by one half for a given wavelength, then the antenna diameter must be doubled. Figure 12 shows antenna diameter as a function of beam width.

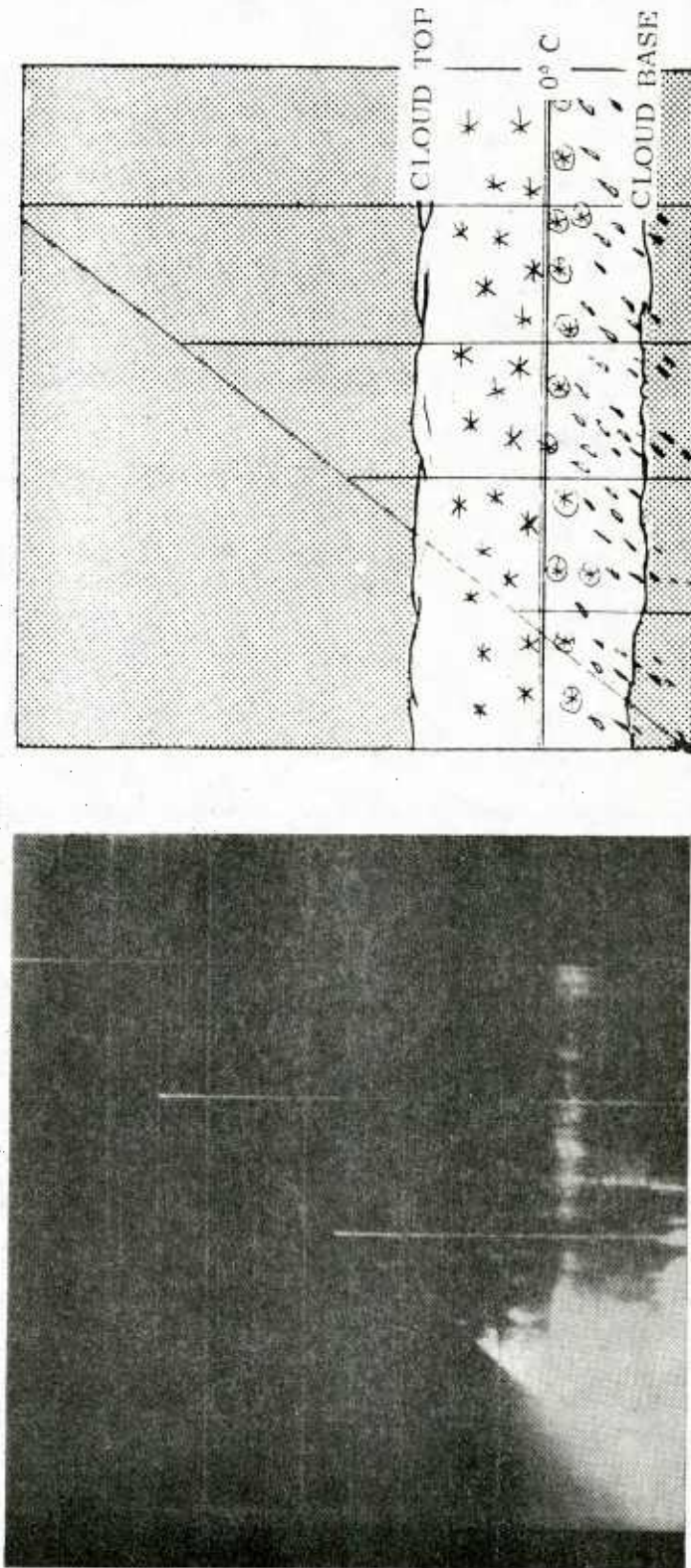


Figure 10. The drawing on the right illustrates the weather conditions that produced the RHI display seen on the left. The snow in the upper regions of the cloud was not detected by the radar, but as it fell into warmer regions and began to melt, it became water coated and had high reflectivity. When it became completely melted near the base of the cloud, its reflectivity decreased. The drops were small, and very little precipitation reached the ground.

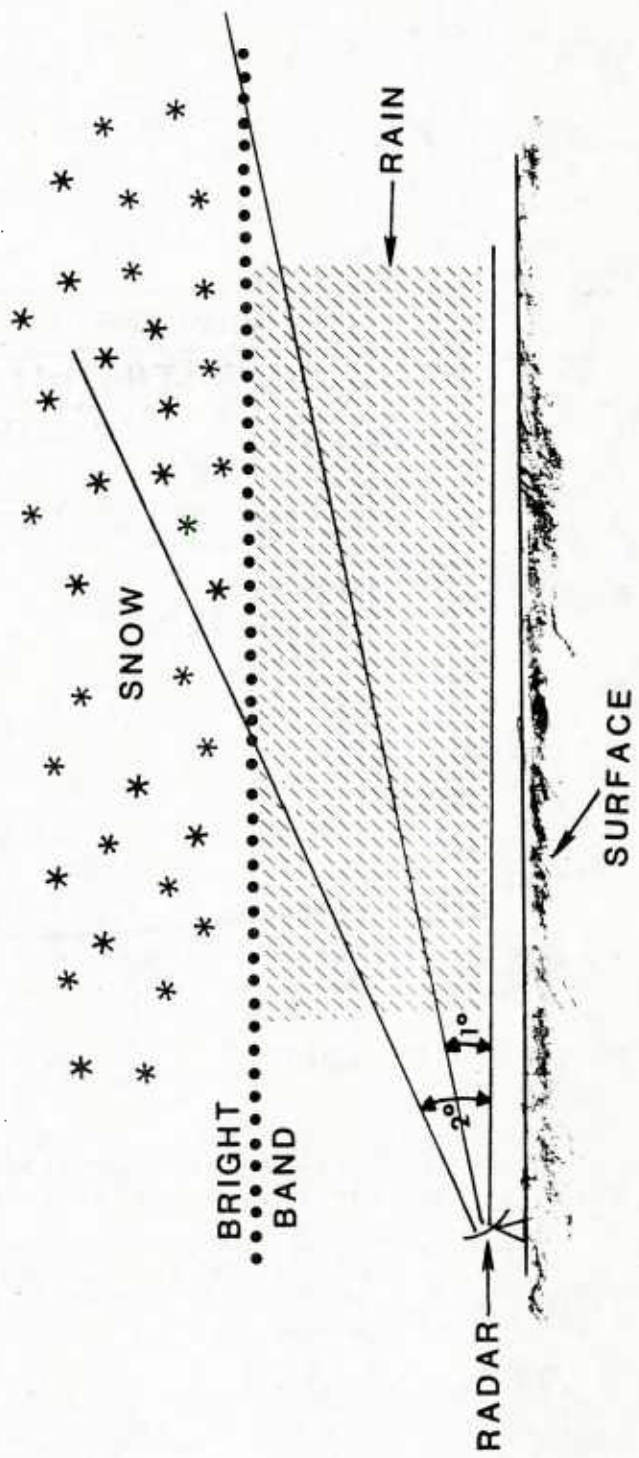


Figure 11. Effect of increased beam width on the range to which precipitation can be measured in the presence of a bright band. As the beam width is increased, the range at which the beam intercepts the bright band decreases. Since the bright band distorts rain measurements, the range to which rain measurements can be made also decreases.

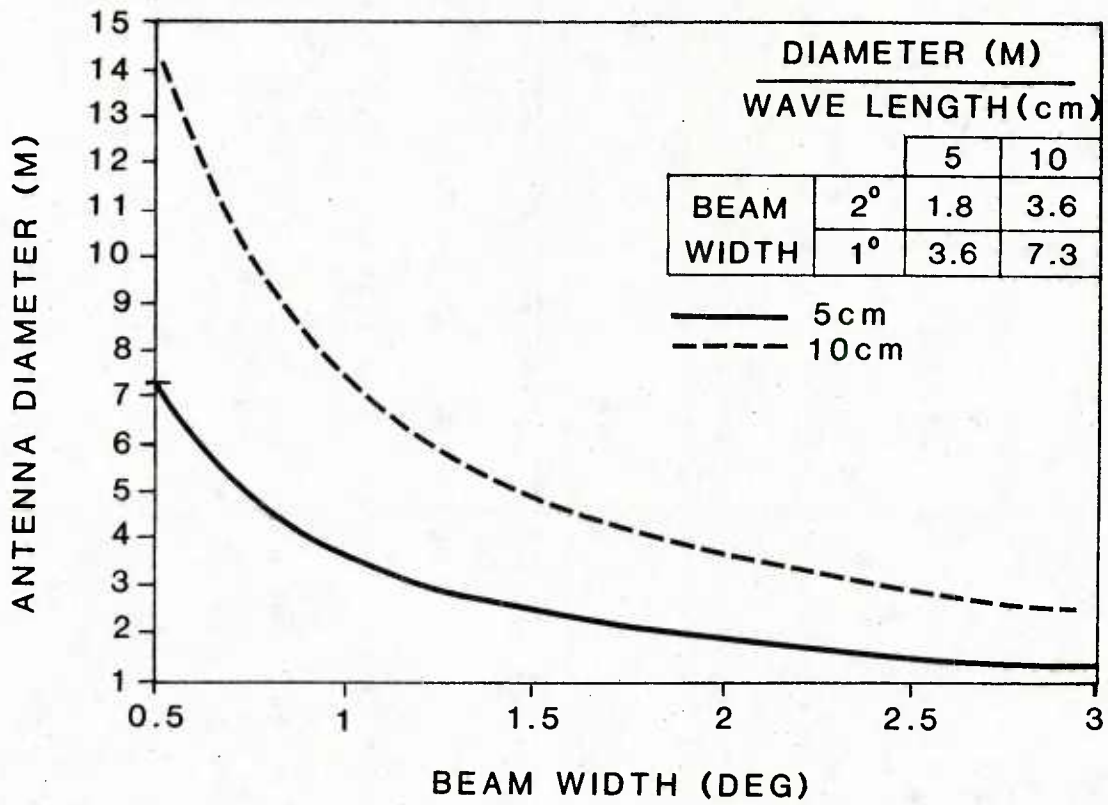


Figure 12. Plot of the relationship between antenna diameter and beam width. The table at the top are values taken from the graph.

3.2 Pulse Length/Range Resolution

The returned power increases as pulse length increases. This increase in returned power is at the expense of range resolution since pulse length is inversely proportional to the number of independent range cells per kilometer of range. If the pulse length is too large, significant features can be smoothed out and missed just as with increased beam width. What constitutes a significant feature depends on the application of the meteorological radar. For non-Doppler data, the pulse lengths typically are between $0.8 \mu\text{s}$ (250 m) and $3.3 \mu\text{s}$ (1 km). For Doppler applications the pulse length should be less than $2 \mu\text{s}$ (600 m).

The variation of radial velocity of the different scatterers within the pulse volume tends to increase as the pulse length (and hence pulse volume) is increased. This results in a broadening of the Doppler spectrum, and therefore increases uncertainty in the estimate of the mean velocity.

One disadvantage of short pulse lengths is the increase in the amount of data that must be processed. For a given maximum range, halving the pulse length doubles the amount of data. Another disadvantage is that to maintain the same sensitivity for a given PRF, as pulse lengths are shortened, the peak transmitted power must be increased. The increase in transmitted peak power can be mitigated to some extent by the use of complex wave forms and pulse coding which increases system complexity and cost.

3.3 Transmitted Power

If other radar design parameters are held constant, then for a given range, the minimum backscatter cross section that can be detected is inversely proportional to the transmitted power (Eq. 6). If a given receiver can detect a -8 dBZ return at 50 km with a transmitted power of 1 MW, it would only be able to detect a -5 dBZ return with a transmitter power of 0.5 MW.

Stated another way, if the transmitted power is halved for a given receiver sensitivity, then the maximum range to which effective precipitation measurement can be made is reduced by $\sqrt{2}$ (Eq. 7). Typical transmitted powers for meteorological radars are 250 KW for 5 cm radars and 1 MW for 10 cm radars.

Two methods for maintaining sensitivity at low transmitter powers are to increase the sampling time and/or to increase the pulse length. Both have their drawbacks. Sampling time is increased by averaging over a larger number of pulses. This means that the radar must look along each radial longer which causes the antenna to rotate slower and, thus, takes longer to scan a given area. An increase in pulse width will result in a decrease in radial resolution as previously discussed.

3.4 Frequency

As previously discussed, meteorological radars typically operate in the 3 to 30 GHz frequency range. This is because, above 30 GHz, the attenuation due to water vapor and precipitation is significant and limits range and accuracy. Below 3 GHz the sensitivity to precipitation decreases limiting the radars usefulness as a meteorological instrument. The physical size of the antenna also becomes a problem. Most operational meteorological radars are at either 3 or 6 GHz. 3 GHz is preferred as it is attenuated less by precipitation. 6 GHz is considered the highest frequency for precipitation measurement. Significant attenuation can occur even at 6 GHz in very heavy precipitation resulting in erroneous measurements. If the detection of clouds in a precipitation free region is of concern, then a frequency near 30 GHz should be chosen.

The choice of frequency also affects the diameter of the antenna. If the same beam width is maintained and the frequency is doubled, then the required antenna diameter decreases by half.

The choice of frequency also affects the unambiguous velocity. This was discussed in Section 2.2 and illustrated in Figure 6. If the frequency is doubled, the unambiguous velocity is cut in half.

3.5 Polarization

Radars designed to measure precipitation typically are horizontally polarized. This is because rain drops tend to be oblate spheroids and returns for horizontally polarized radars are larger than for other polarizations. Therefore, preference should be given to radars that are horizontally polarized.

A dual polarization radar (horizontal and vertical polarizations) might be considered in light of the possible improvement in precipitation estimation (see Section 2.1.1.2). Even though still experimental, confidence in this approach is increasing and could shortly be considered suitable for operational applications given suitable radars.

4. CURRENT CAPABILITIES

Current meteorological radars employing digital processing have greatly expanded capabilities over their predecessors (Bjerkass and Forsyth, 1980). These enhanced capabilities do however require a well calibrated radar system. Meteorological radar displays now incorporate color, thereby making their interpretation easier even though more information may be included. The following discussion is divided into two sections according to whether intensity or velocity data is being addressed.

4.1 Intensity Data

As with previous radars the intensity display still contains much information. With digital processing and color, the display is no longer limited to six contour levels and the contour levels can be easily changed. This can be desirable when looking at winter storms where the intensity range is not as great as with summer storms. Thus, storm detail could be lost using the same contouring levels for all cases. The color contour levels are also easier to read and there is less chance for error. With contoured displays the structure of the precipitating system is easier to discern. Regions of high reflectivity (high rainfall

rate) can easily be determined and tracked. Figure 13 is an example of a color-contoured intensity PPI (Plan Position Indicator) display of an approaching squall line. In the figure, the red areas indicate regions of extreme rainfall rates and the possibility of hail.

With digital processing of the data, additional information can be extracted using various algorithms. Table 5 presents a list of algorithms that exist or are under development. Many of these algorithms were developed in support of the NEXRAD program. Several of the algorithms require complete volume scans of the storm. These algorithms are discussed in turn below.

Table 5. Algorithms using meteorological radar intensity data.

- Storm tracking
- Storm position forecast
- Storm structure
- Vertically-integrated liquid water
- Hail
- Severe weather probability
- Precipitation rate
- Transverse wind

There are several versions of storm tracking algorithms available (Brasunas, 1984). The simplest tracks the maximum intensity return. Another tracks the storm centroid. The best method to use appears to depend on the type of storm being tracked. Independent of the method used, forecasts of the storm movement can be made and plotted on the display along with the storms past track.

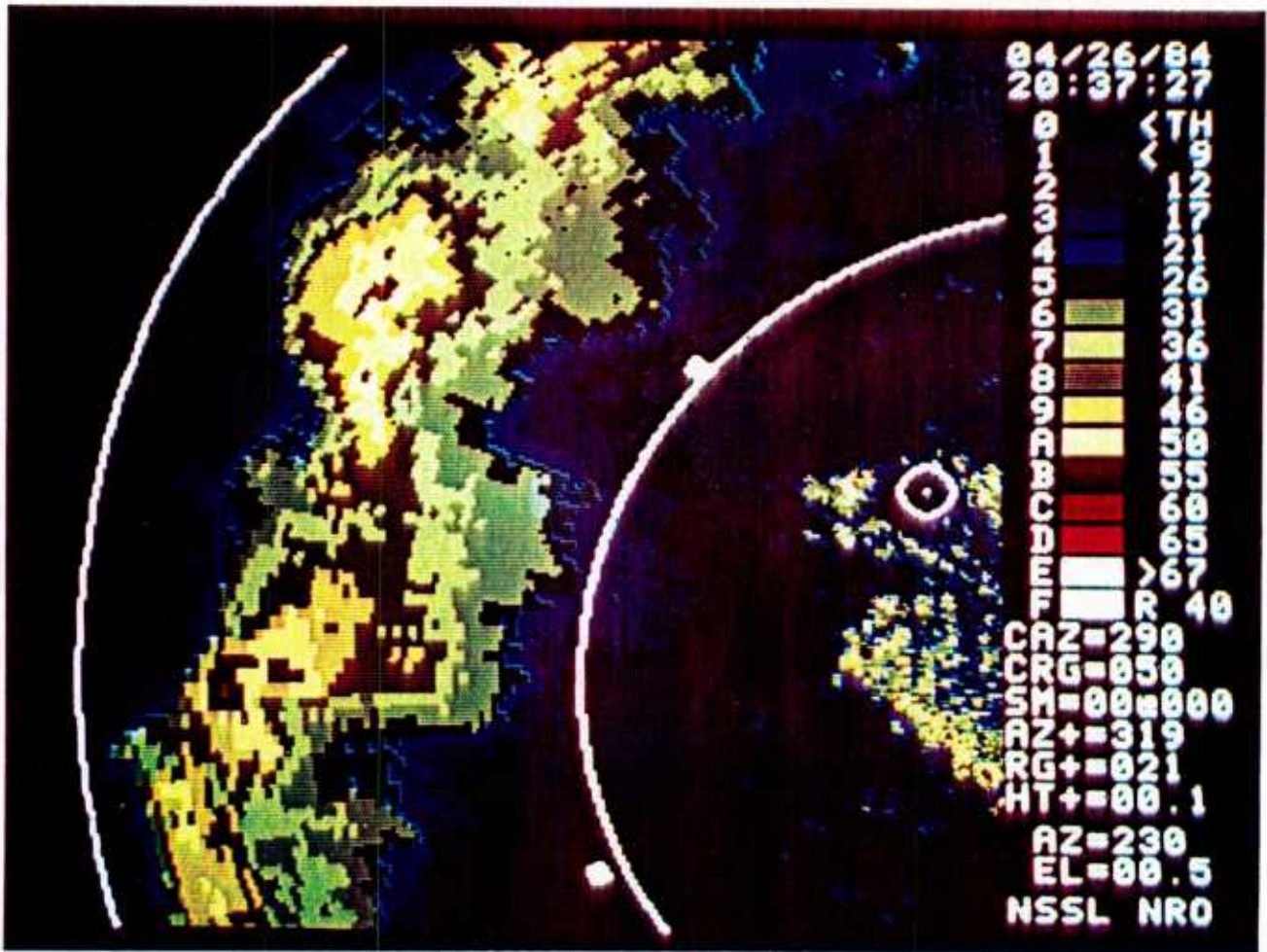


Figure 13. Example of contoured intensity display. The display is of an intense squall line to the northwest of Norman, OK, moving to the southeast. The contouring levels indicate the intensity of the return and thereby the precipitation intensity. Photo courtesy of the National Severe Storm Laboratory, Norman, OK.

The storm structure algorithm looks at a three-dimensional region defined as a storm and determines the following parameters:

- * Storm base
- * Storm top
- * Storm volume
- * Maximum storm reflectivity and its altitude of occurrence
- * Storm tilt and its components along horizontal and vertical axes
- * Storm overhang
- * Overhang orientation

These parameters can then be used as input to other algorithms, such as storm severity, or can be tabulated or plotted along one side of the display. For example, a plot of the history of the maximum reflectivity and its altitude would enable a forecaster to monitor the evolution of the storm.

The vertically-integrated liquid water algorithm converts meteorological reflectivity data into liquid water content. The conversion is based on studies of drop size distributions and empirical studies of the relationship between the reflectivity factor and liquid water content. Large values of vertically-integrated liquid water have been correlated to severe thunderstorms. The output from this algorithm is used by the severe weather probability algorithm. The liquid water distributions could also be used to estimate the attenuation field.

The severe weather probability algorithm is used to determine the probability that a given echo is associated with a severe storm. A severe storm is defined as one with a tornado or funnel cloud, surface hail $\geq 3/4$ inch, and/or wind gusts ≥ 50 knots or reported wind damage (NEXRAD JSP0, 1985). The results could then be used to flag storms suspected of being severe.

The precipitation rate algorithm converts meteorological radar reflectivity data to rain rates. The conversion is performed using empirically determined relationships between the reflectivity factor and rain rates and studies of drop size distributions (see Section 2). The output of the algorithm can be plotted on a display or as input to a higher level algorithm dependent on rain, such as one to estimate attenuation at mm wavelengths.

The hail algorithm is used to help identify storms likely to produce hail. The algorithm uses output from the storm tracking and storm structure algorithms. As currently implemented in NEXRAD it is used to identify one of the following cases:

- * a given storm is producing hail or soon will produce hail
- * a given storm is probably producing or will probably produce hail
- * a given storm is not currently producing hail
- * a given storm cannot be analyzed due to lack of sufficient data.

The transverse wind algorithm is used to determine horizontal wind direction and speed. The approach seeks to find similar patterns in the reflectivity field in successive scans at the same tilt (Rhinehart, 1979). The similarity is determined by dividing the initial scan into boxes. Then for each box in the initial scan, the box in its neighborhood in the second scan that has the maximum correlation with it is found. The displacement of the second box from the first is used to define the direction and speed. The output can be used to supplement the radial winds determined by Doppler processing. Figure 14 is an example of a wind field retrieved using this method (Rhinehart, 1982).

4.2 Velocity

If a Doppler radar is used then velocity and spectral width information are also available. Two additional base products and additional algorithms are now available. Figures 15 and 16 are examples of the PPIs of the velocity and spectral width corresponding to the intensity PPI of Figure 13. The additional base products alone add considerable information. In the velocity

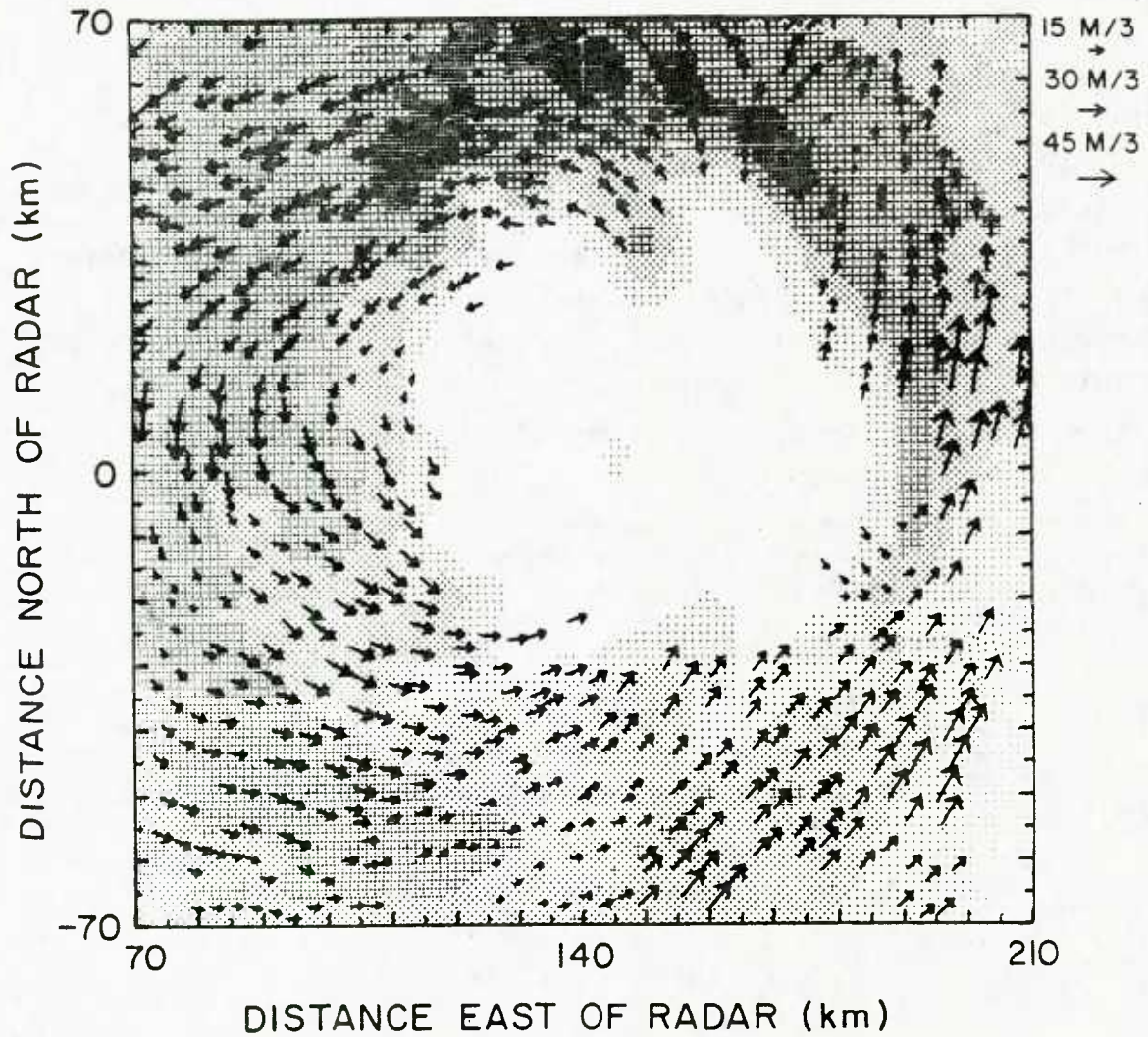


Figure 14. PPI of radar reflectivity data and TREC vectors for Hurricane Frederic collected by the Slidell, Louisiana, NWS WSR57 radar at 0331 UT on 12 September 1979 at 0.8 deg elevation. The shaded regions are reflectivity contours starting at 15 dBz and increases at 10-dB intervals (from Rinehart, 1982).

display of Figure 15, a gust front is seen to be leading the squall line with a peak velocity towards the radar of 28 m/s. The shear across the gust front is 40 m/s. The gust front is in a region of low reflectivity and there is no indication of its presence in the intensity plot of Figure 13. Some idea of the vertical wind profile can usually be determined from the velocity PPI display. The simulated return in Figure 17 indicates wind veering with height, and the closed contour indicates a jet blowing from the southwest to the northeast. Figure 16 is a plot of the spectral width. High values are associated with turbulence. A region of large spectral widths is indicated along the gust front as would be expected indicating increased turbulence. Algorithms that have been or are being developed that use Doppler meteorological information are listed in Table 6. The output from the algorithms can be used directly or input to higher level algorithms or tactical decision aids (TDAs).

Table 6. Algorithms that use meteorological Doppler radar data that have been developed or are under development.

- * Mesocyclone Detection
- * Velocity Azimuth Display
- * Turbulence
- * Tornado Vortex Signature
- * Combined Shear
- * Modified Velocity Volume Processing
- * Divergence Detection
- * Sectorized Uniform Wind
- * Gust Front Detection

The Mesocyclone Detection algorithm is used to detect mesocyclones. A mesocyclone is a horizontally rotating three-dimensional region in a storm. Mesocyclones have been associated with severe weather. The algorithm uses pattern recognition techniques to search the velocity field for symmetric regions of large azimuthal shear. The algorithm can also be used to detect gust fronts parallel to a radial.

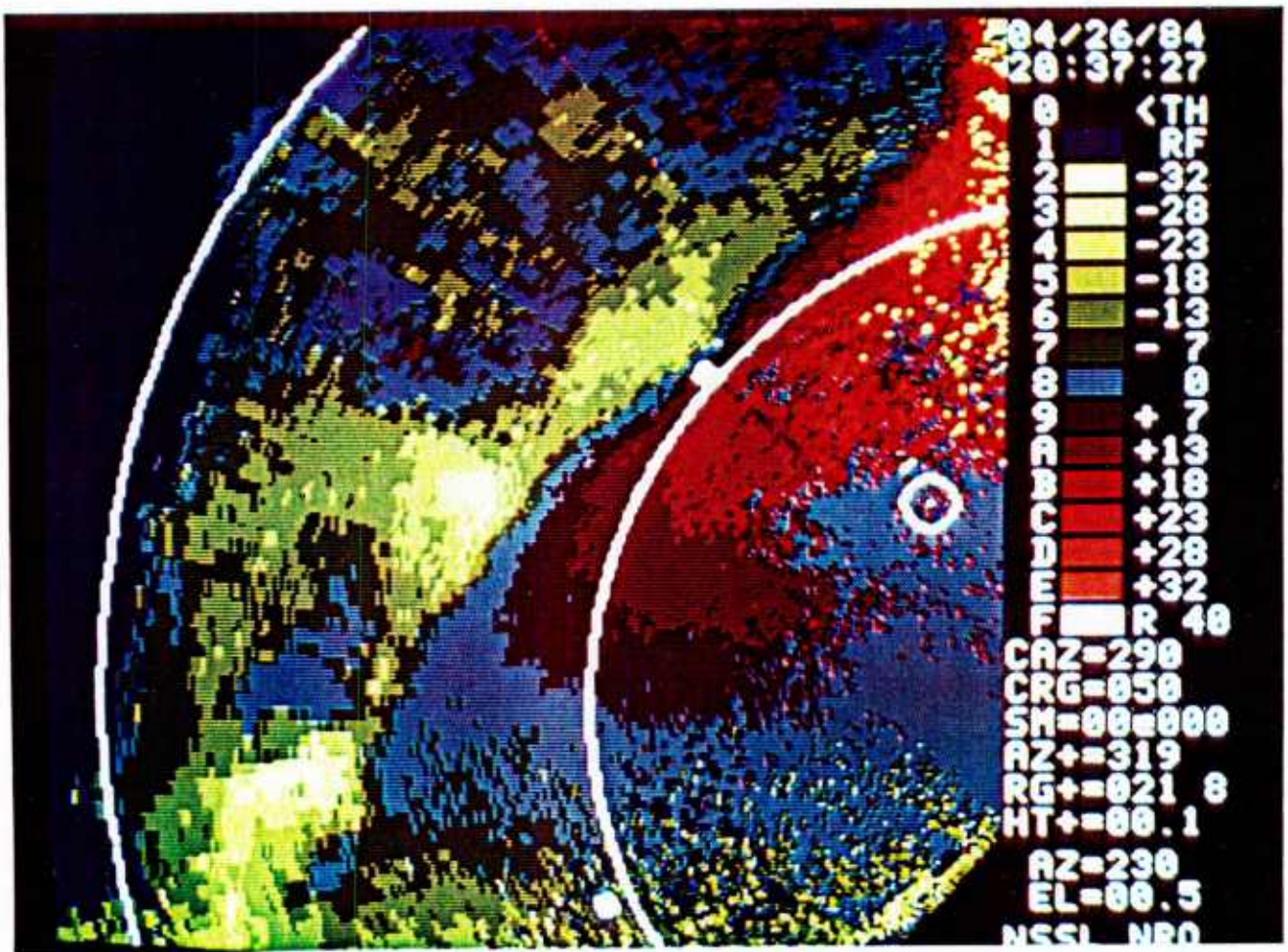


Figure 15. Example of radial velocity information obtained using a meteorological Doppler radar corresponding to the intensity field of Figure 13. Negative velocities are toward the radar and positive velocities are away. A convergence line can be seen to the northwest with a velocity differential of 60 m/s. Comparison to Figure 14 shows that the convergence line is in front of the squall line proper. Photo courtesy of the National Severe Storm Laboratory, Norman, OK.

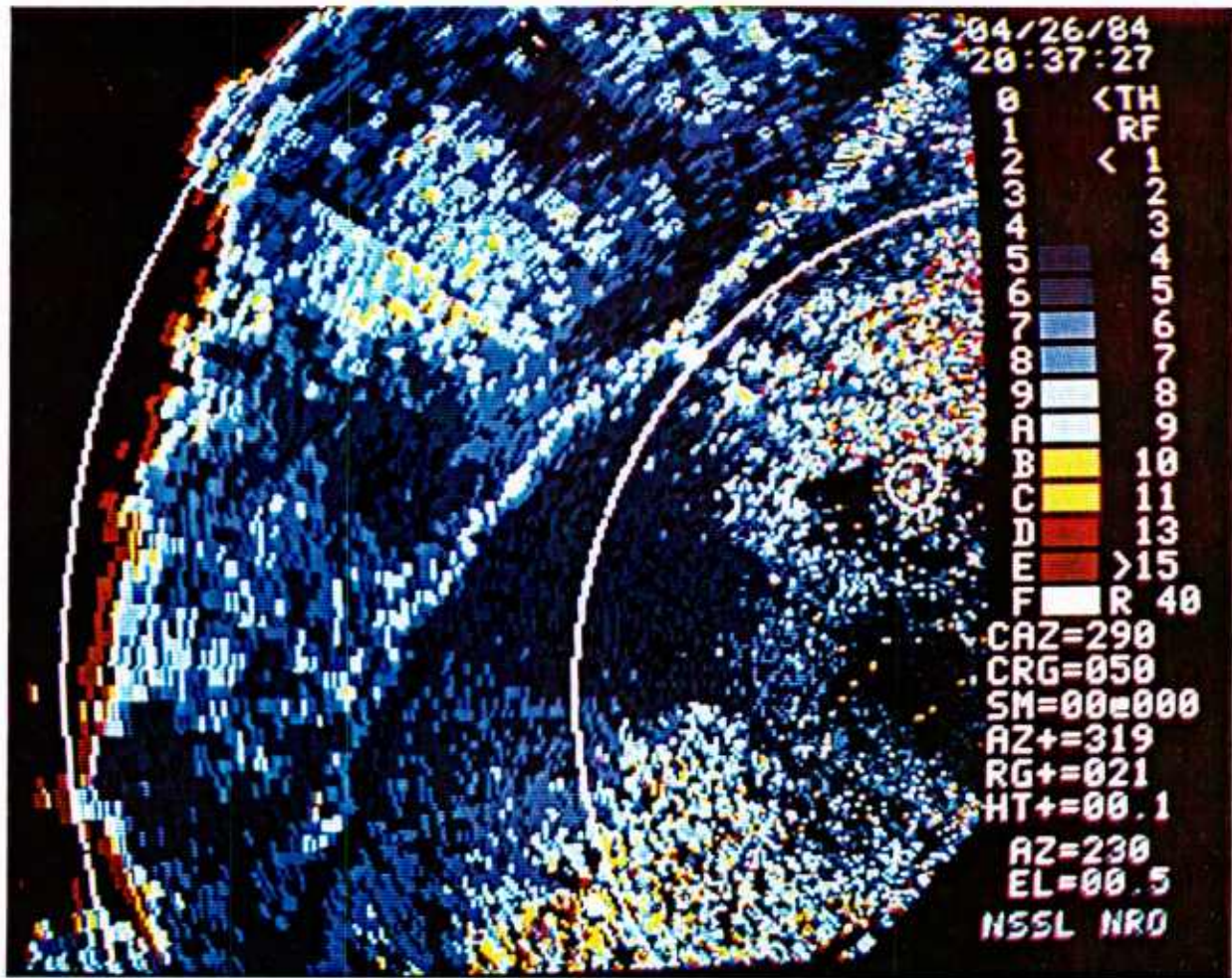


Figure 16. Example of spectral width information obtained using a meteorological Doppler radar corresponding to the intensity and velocity field of Figures 13 and 15. The line extending from southwest to northeast is a region of high spectrum width associated with the leading edge of the gust front. Strong turbulence could be expected along this line.

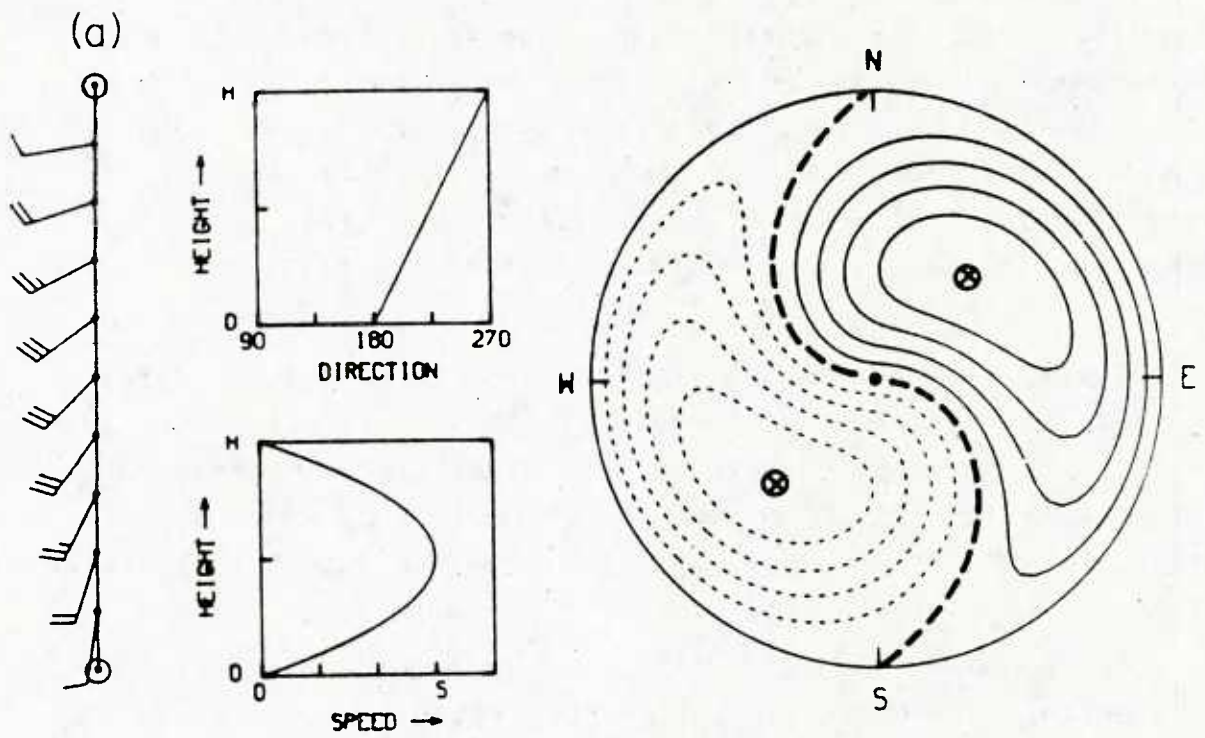


Figure 17. Contours of radial velocity field derived from wind profile at left. The curvature of the zero radial velocity line (heavy dashed line) indicates a veering of the wind with height. The closed contours indicate a jet at mid-level blowing from the SW to the NE. The dashed lines indicate flow toward the radar (from Wood and Brown, 1983).

Velocity Azimuth Display (VAD) processing is used to obtain the vertical profile of mean horizontal wind direction and speed, divergence, and vertical velocity for the region of the atmosphere surrounding the Doppler radar. A harmonic analysis is performed on data collected at multiple azimuths as the radar scans at a constant elevation angle. A sequence of these vertical profiles can be done to provide a time history of the wind profile (Figure 18).

The Turbulence algorithm uses Doppler spectrum variance measurements to estimate the strength of turbulent air motions. Measurements of the radar reflectivity factor and empirical limits of the outer scale of the turbulence for a given meteorological situation are also used. The output is a parameter indicating the presence of light, moderate, or severe turbulence.

The Tornado Vortex Signature (TVS) algorithm is used for the detection of probable tornadic vortices. Tornadic vortices have a distinctive signature on the velocity PPI; however, when viewing a full PPI, it can easily be missed due to their small size. The TVS algorithm is an attempt to automate the detection of tornadic vortices. The output is a yes/no flag.

The Combined Shear algorithm determines a value that is related to, but not equivalent to, the total horizontal wind shear. The value is a combination of the radial and azimuthal wind shears as determined for each grid point from the velocity field. The output is a field of shear values that are easily displayed or input to higher level algorithms. The main application of this algorithm will be in aviation where wind shears are important.

The Modified Velocity Volume Processing (VVP) algorithm is a statistical regression method for calculating the vector wind field over the radar's surveillance area. The algorithm assumes that the wind field varies linearly over the volume being processed and best fits the kinematic parameters of the linear wind model to the observed radial wind field. As configured for

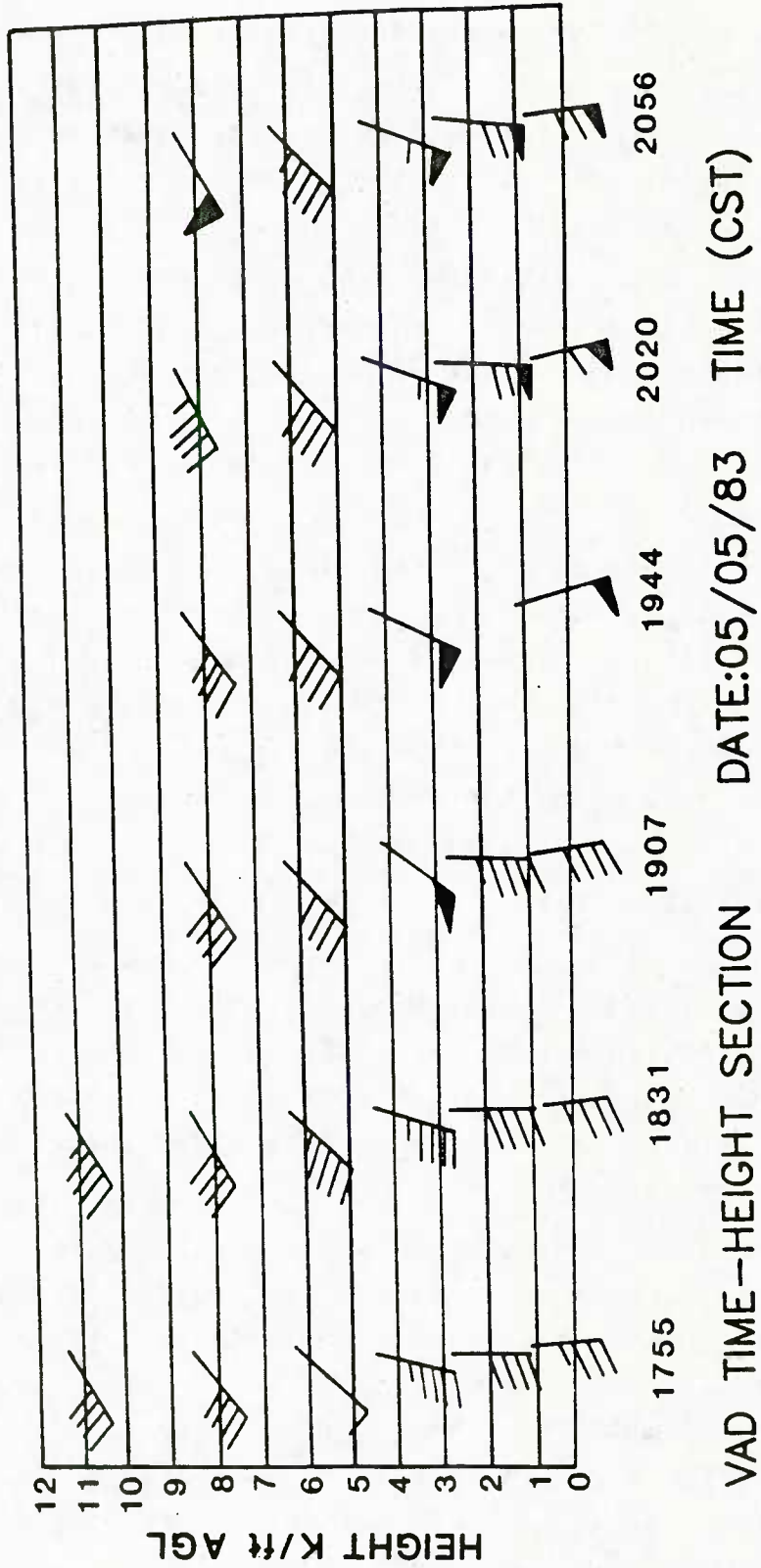


Figure 18. Artist depiction of display of wind profile time history derived from meteorological doppler radar returns. Original display produced by the NEXRAD Initial Operational Test Facility (IOTF) was also color coded.

NEXRAD, the processing volume is 30 degrees by 30 kilometers by two elevation scans. The output is the values of seven kinematic parameters at grid points covered by the processing volume.

The Divergence algorithm is designed to detect divergence in the top of storms. The magnitude of the divergence at the top of storms is related to the severity of the storm. The output is a list of divergence locations and magnitudes.

The Sectorized Uniform Wind algorithm is another method for estimating the transverse wind component. It does this by evaluating the azimuthal derivative of the radial component of the wind. As implemented for NEXRAD the output is composed of wind vectors at 10 degree azimuthal and 7 kilometer radial spacing.

The Gust Front Detection algorithm is used to detect gust fronts not parallel to a radial. Pattern recognition techniques are used to detect the shear lines associated with gust fronts. The outputs of the algorithm describe the gust front as to location and strengths. The gust front in Figure 15 would be detected by this algorithm and the appropriate action initiated, such as the sending of an alert message.

4.3 Returns In Optically Clear Air

Up to this point the discussion has been limited to returns when hydrometeors were present in the sample volume to produce a return. Returns have also been observed in the optically clear air by radars operating at frequencies from 10 GHz to 50 MHz. The source of the returns has been subject to some debate, especially at frequencies above 3 GHz.

The principle sources of returns in the optically clear atmosphere are 1) refractive index variation, and 2) insects and birds. The refractive index variation is the result of turbulence at scales of $L/2$ (L = wavelength). If the $L/2$ scale is within the inertial subrange of turbulence, then echoes can be detected. If the $L/2$ scale is within the viscous dissipation range, however, the turbulence is rapidly damped and the radar reflectivity decreases.

The returns for radars operating in the 50 MHz to 900 MHz range are normally attributed to turbulence induced refractive index variation. Several radars have been developed in this frequency range to observe vertical wind profiles mainly above the boundary layer (Zamora and Shapiro, 1984; Larsen and Röttger, 1982; Balsley and Gage 1982). These radars are known as UHF/VHF profilers. Figure 19 is an example of a wind profile time history obtained using a wind profiler. Sampling rates as high as one profile per minute are obtainable, but longer averaging times are usually used.

Antenna size is a problem with these systems. At 50 MHz the antenna is typically a phased array between 50 and 100 meters on a side. As the frequency increases the antenna size decreases and at 900 MHz a 3 m antenna may be sufficient, depending on the required attitude range.

The height to which observations can be taken consistently is also influenced by the radar frequency. The lower frequencies should be able to go to higher altitudes because their critical turbulence scale is larger than for the higher frequencies.

For meteorological radars operating in the 3 to 6 GHz frequency range there is considerable debate over whether the observed clear air returns are due to refractive index turbulence or to insects and birds, or both. Kropfli (1984) reported X band returns in the optically clear air and attributed the returns to particulate scatterers. He said that there was evidence that they were "not 'strong fliers' if, in fact, they are flying insects at all." Hennington et al. (1980) presented calculations and some observations that indicate that a 3 GHz Doppler radar could at times detect clear air returns. Doviak and Berger (1980) using dual Doppler methods were able to reconstruct the spatial structure of planetary boundary layer air motions. They concluded that the refractive index structure constants C_n^2 deduced by radar and aircraft were within 1 dB. This would seem to indicate that the primary source of returns was refractive index turbulence at least for their daytime conditions.

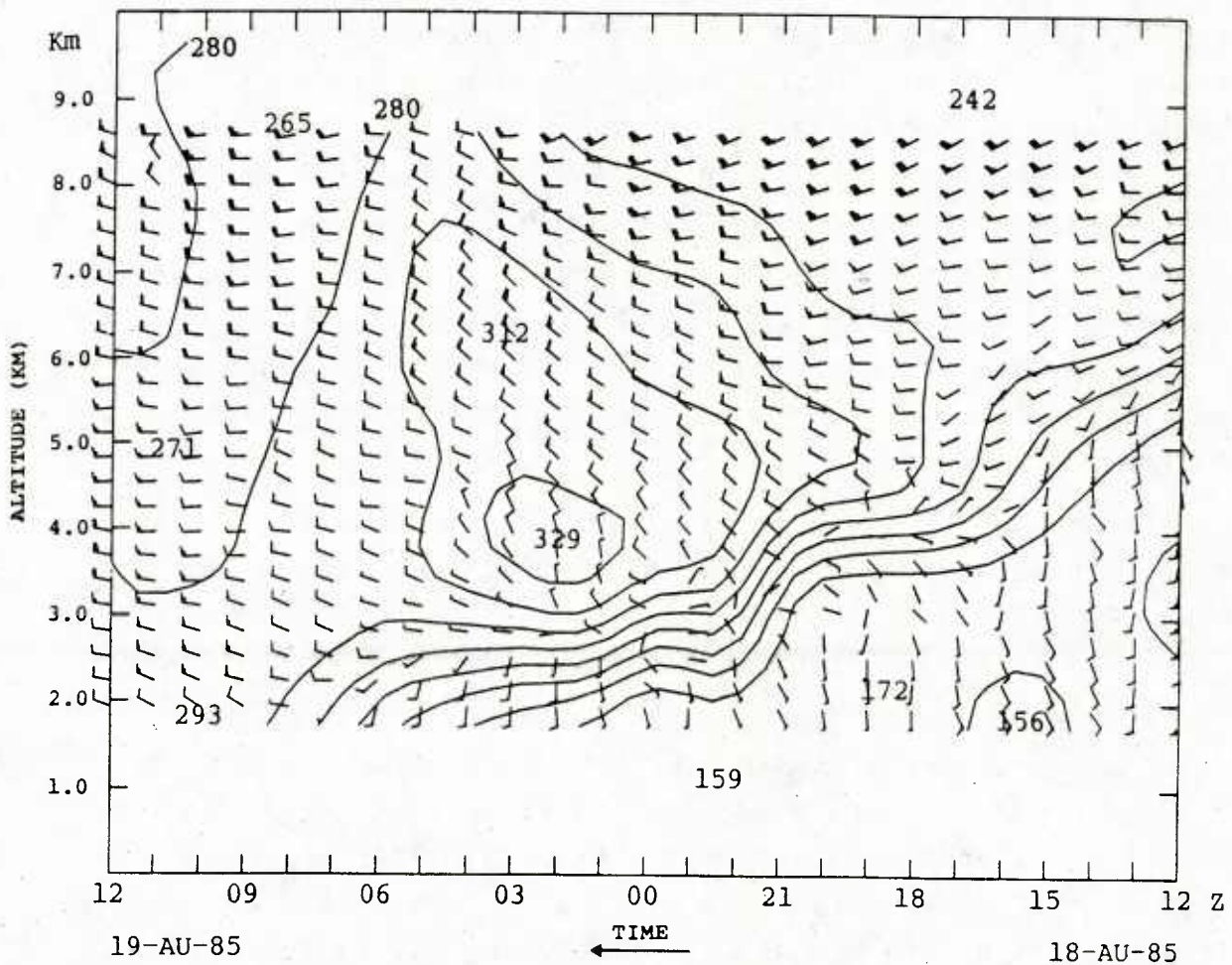


Figure 19. Time-height sector of hourly average profiler winds recorded using the Pennsylvania State University Shanty Town 59 MHz radar. Time periods is from 12 GMT 18 August (RHS) to 12 GMT 19 August (LHS) 1985. Major ordinate divisions are km, msl. Radar site altitude is approximately 400 m. Isopleths are of wind direction in 20° increments and vertical resolution set to 300 m. The section shows a cold front passage associated with the remnants of Hurricane Danny as the system passed over Pennsylvania.

Almost all of the clear air measurements for both UHF/VHF wind profilers and meteorological Doppler radar have been made over land or along a continental coast. What the results would be over the open ocean is uncertain. It is believed that there should be little effect on UHF/VHF profilers; however, with Doppler radars operating in the 3 to 6 GHz range, there is more uncertainty. It is not known whether they would be able to detect clear air returns over the open ocean. And if they can, what percentage of the time would they be able to, and to what height. These questions can only be resolved by field programs to collect both UHF/VHF profiler and conventional Doppler meteorological data at sea.

5. CURRENT METEOROLOGICAL RADAR STATUS IN THE NAVY

Currently the Navy has only one radar designed for meteorological use (the FPS-106) that is used exclusively at ashore locations. Many Naval Oceanography Command detachments do not have a radar unit. A few mobile units are assigned to Marine Air Corps Squadrons for use by assigned weather personnel. Most of the remaining detachments in the continental U.S. have a tap off a nearby National Weather Service Radar using a RADIDS (Radar Information and Display System) unit.

The RADIDS unit is a remote digital color display. The user has the capability to dial up any National Weather Service radar with RADIDS and obtain their current display. The user has no choice in the scan sequence or the area scanned, or the nature of the display. The display is contoured with six colors corresponding to the National Weather Service six intensity levels (see Table 2).

The FPS-106 is a 5 cm (6 GHz) radar with either a 1.5° beam width (fixed installation) or a 2.0° beam width (mobile installation). The mobile units are used by weather personnel assigned

to Marine Corps Air Squadrons for support. The radar has a transmitted power of 3000 kw. The receiver is not calibrated and only relative storm intensities can be obtained. It cannot be determined, for example, how heavy the precipitation is, only that one portion of the storm is precipitating more than another portion. Also the display is not contoured. Contoured displays have been the practice with most weather radars for many years and the lack of contouring further reduces the utility of the radar. A contoured radar display generated using calibrated data gives a better depiction of the storm structure. This allows the operator to better monitor storm development and movement for improving warnings, the directing of aircraft, etc.

Storm motion is determined by plotting storm position on the screen for successive scans as is done with most meteorological radars; however, because of the lack of contouring, only the general storm movement can easily be tracked. The motion of stronger individual cells embedded within a larger system are much harder to track. Also, unlike other radars there is no parallax error correcting feature. This can lead to significant error in determining storm motion. Parts for the FPS-106 are also hard to obtain, making maintenance and reliability a concern.

The only meteorological radar information available afloat is from tactical radar displays or repeaters connected to the tactical radar displays. A Typical radar used is the AN/SPS-48. The meteorological user has no control over the scan sequence, any of the radar parameters, or the data processing. The output is again uncalibrated and not contoured. Since precipitation returns are considered to be noise by the tactical radar user, they often try to eliminate them from the display further reducing the meteorological usefulness. When tactical radars aboard ship are available for meteorological use, they are often considered to be useful even with the above limitations.

Both ashore and afloat, the principal meteorological application of the radar is in support of the forecast office nowcasting efforts. With the current limitations of the available meteorological radar data, this consists mainly of determining storm position, speed, and direction of movement. Only coarse estimates of storm severity can be made. Some installations also use meteorological radar information to route aircraft around storms.

6. IMPLEMENTATION OF RADAR METEOROLOGY IN THE NAVY

6.1 Ashore Installations

In the continental U.S., most Naval Oceanography Command detachments and Marine Bases with Marine Air Corps Squadrons will have access to the products discussed in Section 4 through NEXRAD Principal User Processors (PUP). The PUP is an interactive user interface to the NEXRAD system which allows the user to request, display, and store the various products from any NEXRAD radar site. The PUP unit can also annotate and redistribute the product. The displays are in full color. Some overseas naval bases located near air force bases with NEXRAD units will also have PUPs. The remaining overseas bases and the mobile FPS-106s do not currently have any replacements scheduled.

Because the FPS-106 is old and parts are hard to obtain, it is due for replacement. Support radars for overseas sites and for mobile support of the Marine Corps Air Squadrons are still needed. Therefore a replacement meteorological radar system will need to be developed. It should be possible to fill both needs with different models of the same basic radar system as did the FPS-106.

The new meteorological radar should incorporate Doppler radar and advanced digital processing technologies. As these radars will be providing weather information for flight planning and safety and base safety, the majority of the NEXRAD type algorithms would be applicable and should be included. As an absolute minimum, displays of echo intensity and velocity fields

must be included. Without the velocity fields, important features such as gust fronts, wind shift lines, and wind shears will be missed.

When choosing a replacement radar, a choice of operating wavelength must be made. A 10 cm (3 GHz) radar is preferred. It is attenuated less by precipitation than a 5 cm (6 GHz) radar, resulting in better rain rate estimates and a reduced chance of shadowing one storm by another. Reasonable rain rate estimates can be obtained from a 5 cm radar, except at extreme rainfall rates. Shadowing is also a major problem only at very high rain rates.

From Section 2 another advantage of a 10 cm radar is that, for a given pulse repetition rate (PRF), it has a higher unambiguous velocity than a 5 cm radar. The disadvantage of the 5 cm system, however, can be mitigated to some degree by the use of multiple PRFs to unfold the velocity field.

When it comes to mobility, however, 10 cm radar systems tend to be less mobile than a 5 cm radar systems. Both the transmitter and antenna are larger for the 10 cm radar. For a given beam width, the antenna for a 10 cm system is twice as large as for a 5 cm system. The smaller size of the 5 cm radar system components would also be an advantage for a mobile system. The reduction in antenna size would also reduce its cost.

Another question that has to be addressed is the choice of beam width. From previous sections we know that the beam width is important for several reasons. The choice of beam width effects the spectral variance, the size of the sample volume, the resolution, and rain rate estimation. From earlier discussions, a 1.0° beam width would be best based on these criteria alone. But if the velocity estimates were to be made within a 70 nm range, and turbulence and other measurements dependent on spectral width were confined to within 35 nm, then a 1.5° beam width would suffice. For a 5 cm radar the difference in antenna size for a 1.0° vs. 1.5° beam width is 12 ft vs. 8 ft. For a 10 cm system the range is 24 ft to 16 ft.

A suitable pulse length also needs to be chosen. Based on previous sections, a pulse length of 500 m would be recommended giving a range resolution of 250 m. This is short enough to obtain good Doppler information, yet not so small that the amount of data would present a data processing problem.

Based on the need for a mobile system and cost, a 5 cm meteorological Doppler radar system would be recommended. It should have a 1.5° beam width, a 500 m pulse length, a peak transmitter power of 300 kw minimum, and use multiple PRF's to extend the unambiguous velocity.

The complete system would require additional items that would need to be developed. These are antenna controller, signal processor, data processing system, and display generator. A detailed discussion of each of these is beyond the scope of this report; however, a brief discussion follows. The antenna controller is required to control the antenna, and is probably the least costly of all the components. The signal processor takes the signal from the radar receiver and extracts the intensity and Doppler information from it. The data processing system takes the output from the signal processor and applies various algorithms to produce the required output. The complexity of the data processing system depends on the required output. In its most basic form, it would do error checks on the data and format it for output to the display generator. In this case, the only products would be displays of the base variables: intensity, velocity and spectral width. The display generator would take the requested output from the data processing system and generate the display.

6.2 Afloat Installations

There are currently no plans to improve or expand the meteorological radar services afloat. A recent survey of environmental requirements for the Battle Force Information Management system (BFIM) (Space and Naval Warfare Systems Command) summarizes parameters required by a selected subset of

BFIM component systems. Figure 20 summarizes those parameters that can be measured by Doppler radar that are important to the systems surveyed. Not only can radar measure these parameters, it can also often give a 2-D or 3-D picture of the parameter. As the systems surveyed represent only a subset of impacted systems, it is apparent that meteorological radar information would be of great benefit to the afloat community.

PROGRAM	SIGIFICANT Wx (severe storms)	WIND SHEAR/ LOW LEVEL JET	WIND SPEED	TURBULENCE	PRECIPITATION
ACDS	C	R	R	R	R
AEGIS	C		C		R
ASWCS	C		C		M
ASWM	C				M
E-2C	C				
EWCM	C		C		C
FDDS	C	C	C	C	C
ACS	C		C		C
TWCS	C		C		C

C-Critical R-Required M-Marginal

Figure 20. Summary of environmental requirements for each BFIM system included in survey that can be measured using Doppler radar. Extracted from "Report on Environmental Requirements for the Battle Force Information Management System" by Space and Naval Warfare Systems Command.

Many of the products and algorithms described in Section 4 can be of use to the afloat community in their current or modified form. The output from the algorithms can be used directly as input to TDAs. The precipitation fields can be used in the development of a TDA to define areas of good, marginal, and poor target detection and tracking conditions for various tracking methods. Storm tracking algorithms can provide forecasts of storm motion to predict storm position relative to the fleet. The storm position forecasts can also be used to forecast the evolution of detection and tracking conditions. Storm intensity estimates and time histories can be used in tactical planning and/or for ensuring the safety of the fleet.

Doppler wind information can be used to determine the local wind field. Wind shift lines such as fronts and gust fronts can be identified and approximate strength determined, thereby allowing appropriate action to be taken. If a carrier is launching an aircraft, advance notice of a wind shift will reduce downtime while the ship is repositioned. Wind and precipitation also affect cruise missile launch and flight performance. This information obtained from meteorological radar processing can be incorporated into weapon control systems for pre-launch planning. Local wind fields might also be used as an input to sea clutter models allowing for real time updating of the sea clutter model and resulting thresholds. Derived vertical wind profiles can be used as input for programs such as ballistic winds, radiation fallout, etc.

Displays of turbulence fields can be used to increase air safety by routing aircraft around regions of strong turbulence. These regions can also affect the launch of cruise missiles and the missiles can be routed around regions of known strong turbulence.

If clear air returns in the boundary layer can be detected, the times when various wind algorithms can be utilized will be increased. Wind shift lines, wind profiles, turbulence

estimates, etc., could then be made in the absence of precipitation. UHF/VHF wind profilers would add the capability to obtain frequent wind profiles for input to TDAs and numerical models. The wind profiles would also be of value to single station forecast models.

The meteorological Doppler radar data can be processed and sent directly to affected BFIM component systems and/or input to the Tactical Environmental Support System (TESS) where further process could be performed. Figure 21 is an information flow diagram for meteorological radar data to the afloat community.

6.2.1 New Radar

The largest obstacles to the addition of a meteorological radar aboard ships are space and cost. Both spaces for the antenna and the transmitter/receiver/signal processor are at a premium; however, the option should be examined.

The same arguments presented in Section 6.1 in the discussion on a replacement for the FPS-106 meteorological radar are applicable here. Size, however, is of even more importance, making a 5 cm radar system even more attractive. The recommendation is for the same basic system as for the FPS-106 replacement. Two benefits of using the same basic system ashore and afloat are that a common spare parts inventory could be maintained and users would only need to be familiar with one basic system instead of two. The antenna controller will be more complex to compensate for ship motion to maintain antenna stability. Signal and data processing algorithms will also have to allow for ship motion.

The basic system recommended to replace the FPS-106 called for a 5- μ m Doppler radar with a 1.5° beam width, a peak transmitter power of 300 kw, a 500 m pulse length, and multiple PPF's. This would result in an 8-ft diameter dish antenna which would require a 10-ft diameter dome. The transmitter could be housed in a single cabinet and the associated control system, signal processor and analysis system would require another two to four instrument racks.

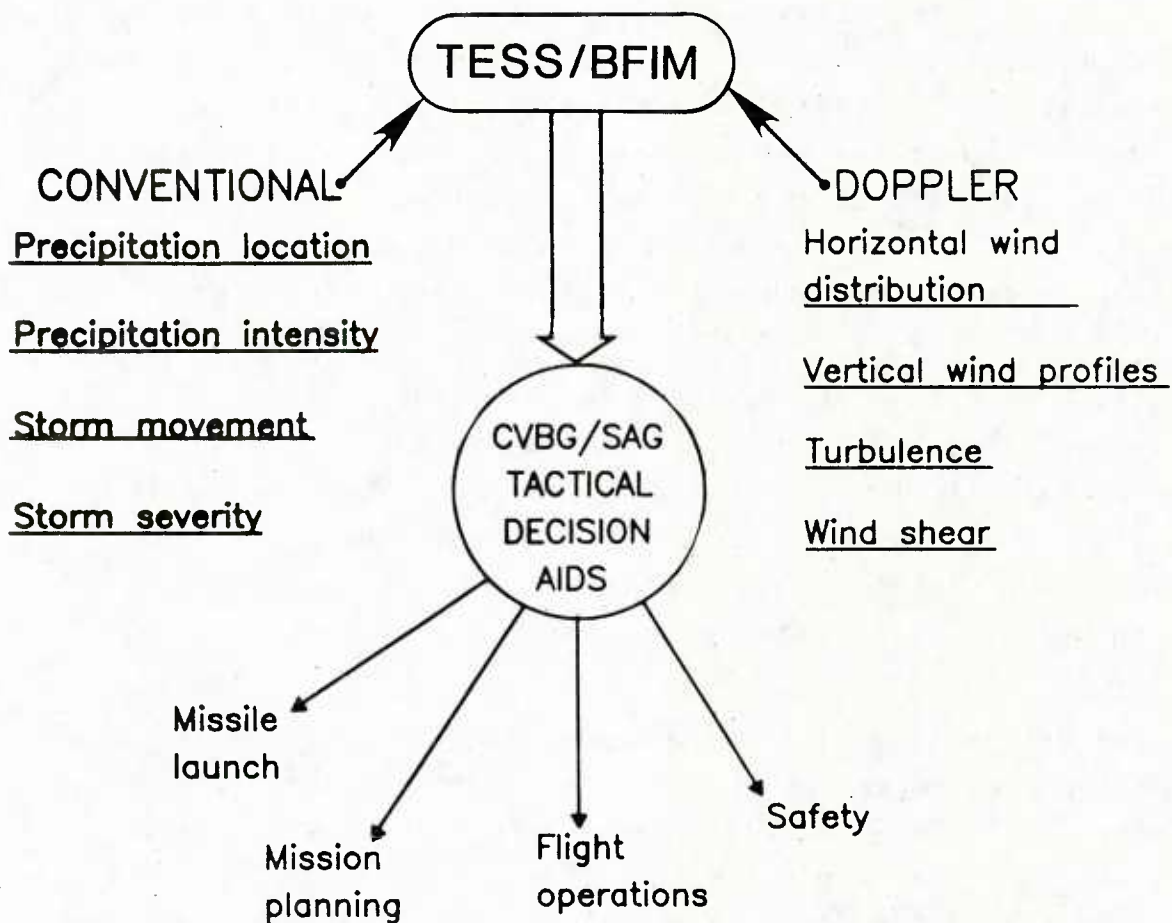


Figure 21. Flow diagram for input of meteorological radar data to the afloat community.

A UHF/VHF profiler would most likely require a new radar system as existing UHF/VHF tactical radars do not have the required beam shape or size. In order to keep the size small, a frequency in the neighborhood of 900 MHz will have to be chosen. This will keep the antenna size in the 3-4 meter range. It may be possible to mount the antenna in a horizontal surface such as the deck or roof. The electronics associated with the profiler does not take up much space.

6.2.2 Existing Tactical Radar

By using an existing tactical radar to obtain meteorological radar information, no new transmitter/receiver and antenna system is required. Any impact on tactical signal processing can be minimized by splitting the received signal and having separate signal and data processors for the tactical and meteorological channels (Figure 22). The signal needs to be split because much of the tactical signal processing removes the information required for the meteorological processing.

Tactical radars are designed for a different objective than are meteorological radars. This results in different choices for the radar design parameters. Fortunately many are somewhat compatible with meteorological applications. The resulting parameter choices for a given radar may not be ideal for all meteorological applications, but at the same time they do not necessarily rule it out.

The examination of the frequency of existing and planned tactical radars reveals that there are several which have frequencies in the 6 and 3 GHz bands. Many of these are eliminated when their beam pattern is examined. A meteorological radar needs a narrow pencil beam, while many of these radars have a fan shaped beam (Figure 23). The beam widths of the remaining radars, while not ideal, would be sufficient if Doppler data acquisition was limited to less than 50 to 70 nm. The pulse lengths are also often reasonable for the extraction of meteorological information. At times they may actually be smaller than required.

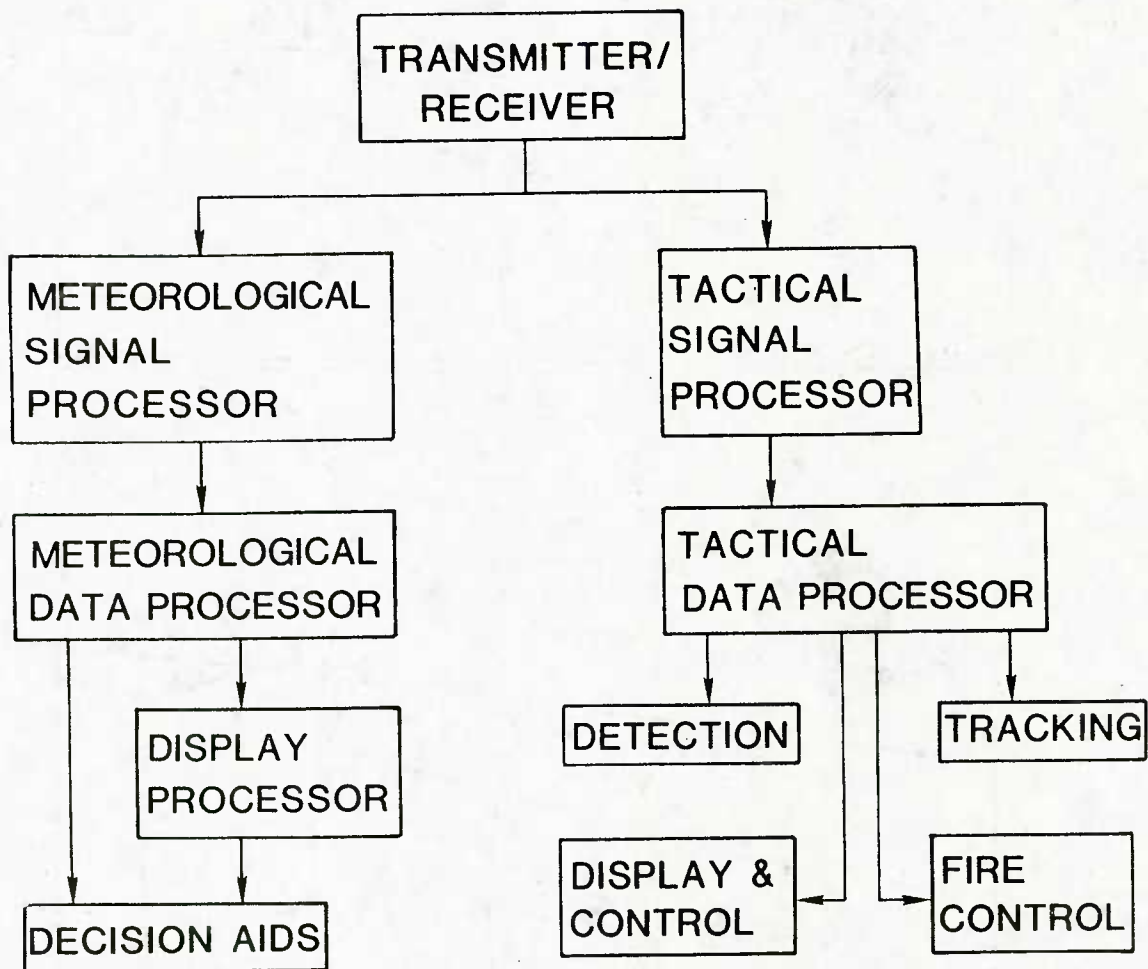


Figure 22. Flow diagram of how the received signal of a tactical radar could be split and fed to two separate processing channels to provide both tactical and meteorological radar information.

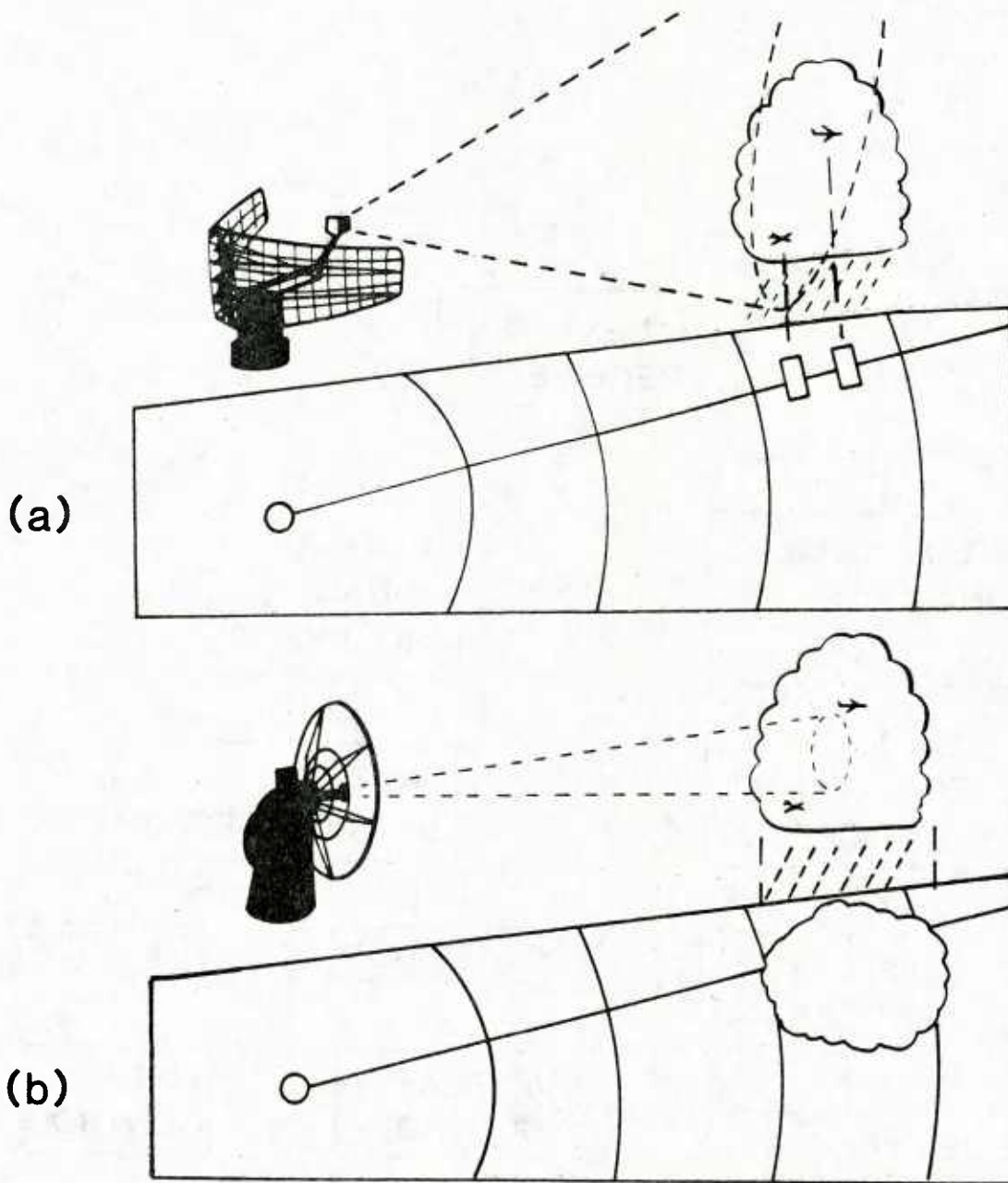


Figure 23. Example of a fan beam (top) used by 2-D search radars and of a pencil beam (bottom) used in meteorological radars and 3-D search radars. The fan beam often is at a frequency not affected by precipitation or has a precipitation canceling circuit.

Many of the tactical radars have the capability to produce a range of pulse repetition frequencies, PRFs. This range often includes PRFs appropriate to meteorological Doppler measurements. At times the PRF may be higher than desired for meteorological measurements, however. The effect of the higher PRFs is to reduce the unambiguous range. If the unambiguous range is reduced too much, the extraction of the information becomes difficult or impossible due to multiple trip echoes (echoes from ranges greater than the unambiguous range). The range corresponding to the data is unknown and multiple echoes can be superimposed upon each other.

The scan rates and dwell times may not be ideal either. Most meteorological radars have a scan rate between 3 and 5 rpm. At higher rpm the dwell times are usually too short to give good estimates of the intensities. The spectrum width is also increased at the higher rpm (see Section 2.2). These problems might be overcome by the use of complex pulse shapes and/or pulse encoding.

On many of the radars a parallel signal and data processing channels could be added to handle the meteorological data processing with minimal if any impact on the tactical data processing. The output from the meteorological processing channel could then be routed to the meteorological station, directed to a BFIM system, or input to TESS.

Earlier it was stated that a fan beam pattern was not suited for the extraction of meteorological data. In the strictest sense this is true; however, MIT Lincoln Labs (Weber, 1985) analyzed the addition of weather processing to the ASR-9 airport surveillance radar. This radar has a vertical fan beam antenna similar to those used on afloat 2-D search radars. The study showed that weather processing could be added to extract rough intensity estimates. The output can be used to locate and track storms. Areas of intense rainfall can also be identified. The apparent structure of the storms is smoothed compared to conventional meteorological radars using a pencil beam. The approach outlined could be adapted to some of the 2-D search radars afloat.

7. SUMMARY AND RECOMMENDATIONS

Meteorological radar information has proven and continues to be useful in land based operations. It could also be useful to the afloat community. The quantitative measurement of precipitation, wind, and turbulence fields could yield useful information that is not now available. Features such as wind shift lines, high turbulence regions, poor target detection regions, etc., could be mapped, followed, and projected. Many of the parameters could be measured as 2-D fields and some as 3-D fields. Some areas in which meteorological radar data could have an impact are target detection and tracking, aircraft launch and retrieval, missile launch, sea clutter modeling, and command and control. The meteorological Doppler radar data and derived information could be passed directly to a BFIM system or to TESS for distribution.

From a meteorological point of view the best implementation would be a radar dedicated to meteorological data acquisition. Since this is not likely, the meteorological data acquisition will have to be piggybacked on an existing or planned tactical radar. A system could be designed such that the meteorological signal and data processing is performed concurrently with any tactical processing. Several existing and planned tactical radars appear suitable. The AEGIS type radar and derivatives appear to be the most suitable. How suitable various tactical radars will prove to be will take additional study.

The following recommendations are made:

1. A link between environmental and warfare communities should be established to pursue meteorological radar data acquisition and utilization. This effort would include the screening of tactical radars for meteorological data acquisition suitability. The screening would incorporate radar design parameters, radar operation, and meteorological requirements. How meteorological Doppler radar data could be incorporated into TDAs would also be investigated.

2. The use of meteorological Doppler radar data to satisfy BFIM and TESS requirements should be examined. Both TESS and BFIM have a need of high resolution data in the vicinity of the battle force for incorporation into TDAs. Meteorological radar is a means of obtaining this data.
3. The FPS-106 radar should be replaced with a Doppler meteorological radar with the capability to measure intensity, velocity, and spectrum width. The capacity to measure velocity is crucial to obtaining optimum utility from a Doppler radar. The additional information obtained with a Doppler radar greatly increases the radar's usefulness.
4. Field programs should be conducted in coordination with ONR to collect meteorological radar data at sea for algorithm development and testing. To date, meteorological data processing algorithms have primarily been developed for land based radars. In order to adapt these algorithms and develop new algorithms for afloat applications, data will need to be collected under operational conditions.
5. The addition of a weather processing capability to 2-D search radars should be investigated. While 2-D search radars are not ideal for acquiring meteorological data, information on storm location, movement, and intensity can be obtained from the returns. This information could be use for aircraft routing and planning purposes.
6. The suitability of UHF/VHF wind profilers for deployment within the fleet should be investigated. Wind profilers could give frequent wind profiles for input to various TDAs and numerical models. Low power models specifically designed to minimize detectability could be developed for probing only the lower atmosphere. This effort would include field programs to investigate the operation of wind profilers in a marine environment.

REFERENCES

- Battan, L. J.; 1973: Radar Observation of the Atmosphere. University of Chicago Press, Chicago Illinois.
- Balsley, B. B. and K. S. Gage, 1982: On the Use of Radars for Operational Wind Profiling. Bull. Am. Meteorol. Soc., **63**, No. 9, 1009-1018, Sept. 1982.
- Bjerkass, C. J. and D. E. Forsyth, 1980: An Automated Real-Time Storm Analysis and Storm Tracking Program (WEATRK). Air Force Geophysics Laboratory, Meteorology Division report AFGL-TR-80-0316, October 1980.
- Brandes, E., 1975: Optimizing rain fall estimates with the aid of radar. J. Appl. Meteorol., **14**, 1339-1345.
- Brasunas, J. C., 1984: A Comparison of Storm Tracking and Extrapolation Algorithms. Lincoln Laboratory MIT Project Report ATC-124, 31 July 1984.
- Crawford, K.C., 1977: The Design of a Multivariate Mesoscale Field Experiment. Ph.D. dissertation, University of Oklahoma, 157 pp.
- Doviak, R. J. and D. S. Zrnic, 1984: Doppler Radar and Weather Observations. Academic Press, Inc.
- Doviak, R. J. and M. Berger, 1980: Turbulence and waves in optically clear planetary boundary layer resolved by dual-Doppler radars. Radio Sci., **15**, No. 2, pp 297-313, March-April 1980.
- Hall, M. P. M., S. M. Cherry, J. W. F. Goddard, and G. R. Kennedy, 1980: Raindrop sizes and rainfall rate measured by dual-polarization radar. Nature (London), **285**, 195-198.
- Hembree, L. and A. Eddy, 1979: "Multivariate Objective Analysis of Convective Complexes," 7th Conference on Inadvertent and Planned Weather Modification, October 8-12, 1979, Bundt, Alberta, Canada.
- Hennington, L., R. J. Doviak, D. Sirmans, D. Zrnic, 1976: Measurement of winds in the optically clear air with microwave pulse-Doppler radar. 17th Conf. on Radar Meteor., NB1, 342-348, October, 1976.
- Jones, D. M. A., 1956: Rainfall drop-size distribution and radar reflectivity. Res. Rept. No. 6. Urbana Meteor. Lab., Illinois State Water survey.

- Kropfli, R. A., 1984: Turbulence Measurements From Particulate Scatter in the Clear Unstable Boundary Layer Using Single Doppler Radar. 22nd Conference On Radar Meteorology, 10-13 Sept. 1984, Zurich, Switzerland.
- Larsen, M. F. and J. Röttger, 1982: VHF and UHF Doppler Radars as Tools for Synoptic Research. Bull. Am. Meteorol. Soc., **63**, No. 9, 996-1008, Sept. 1982.
- Marshall, J. S. and W. M. K. Palmer, 1948: The distribution of rain drops with size. J. Meteor., **5**, 165-166.
- Richards, W. G. and C. L. Crozier, 1981: Precipitation Measurement with C-Band Weather Radar in Southern Ontario. Int. Rpt. No. APRB 112, p. 35, Cloud Phys. Res. Div., Atmos. Environ. Serv., Downsview, Ontario, Canada
- Rinehart, R. E., 1979: Internal Storm Motions from a Single Non-Doppler Weather Radar. Nation Center for Atmospheric Research report NCAR/TN-146+STR
- _____, 1980: Transverse Motion Detection and Hail Detection. Proceedings of the NEXRAD Doppler Radar Symposium/Workshop, P.S. Ray and K. Colbert (eds.), Univ. of Oklahoma, 184-187.
- Space and Naval Warfare Systems Command, 1986: Report on Environmental Requirements for the Battle Force Information Management System (Draft). Warfare Systems Architecture & Engineering Directorate, Space and Naval Warfare Systems Command, November 1986.
- Seliga, T. A., K. Ayden, and V. N. Bring: 1982: Behavior of the Differential Reflectivity and Circular Depolarization Ratio, Radar Signals and Related Propagation Effects in Rainfall. Proc. URSI Comm. F, Open Symp. Multiple-Parameter Radar Meas., pp. 35-42, Rutherford Appleton Lab. Chilton, Didcot, Oxfordshire, U. K.
- Wood, V. T. and R. A. Brown, 1983: Single Doppler Velocity Signatures: An Atlas of Patterns in Clear Air/Widespread Precipitation and Convective Storms. NOAA Tech. Memo. ERL NSSL-95. National Severe Storms Laboratory, Norman, OK., November, 1983.
- Zamora, R. J. and M. A. Shapiro, 1984: Diagnostic Divergence and Vorticity Calculations Using a Network of Mesoscale Wind Profilers. 10th Conference on Weather Forecasting & Analysis, June 25-29, 1984, Clearwater Beach, Fla

DISTRIBUTION

COMMANDER IN CHIEF
U.S. ATLANTIC FLEET
ATTN: FLT METEOROLOGIST
NORFOLK, VA 23511-6001

COMMANDER IN CHIEF
U.S. ATLANTIC FLEET
ATTN: NSAP SCIENCE ADVISOR
NORFOLK, VA 23511-6001

COMMANDER IN CHIEF
U.S. PACIFIC FLEET
CODE 02M
PEARL HARBOR, HI 96860-7000

COMMANDER IN CHIEF
U.S. NAVAL FORCES, EUROPE
ATTN: METEOROLOGICAL OFFICER
FPO NEW YORK 09510

CINCUSNAVEUR
ATTN: NSAP SCIENCE ADVISOR
BOX 5
FPO NEW YORK 09510-0151

COMMANDER SECOND FLEET
ATTN: METEOROLOGICAL OFFICER
FPO NEW YORK 09501-6000

COMSECONDFLT
ATTN: NSAP SCIENCE ADVISOR
FPO NEW YORK 09501-6000

COMTHIRDFLT
ATTN: FLT METEOROLOGIST
FPO SAN FRANCISCO 96601-6001

COMSEVENTHFLT
ATTN: FLT METEOROLOGIST
FPO SAN FRANCISCO 96601-6003

COMTHIRDFLT
ATTN: NSAP SCIENCE ADVISOR
PEARL HARBOR, HI 96860-7500

COMSEVENTHFLT
ATTN: NSAP SCIENCE ADVISOR
BOX 167
FPO SEATTLE 98762

COMSIXTHFLT
ATTN: FLT METEOROLOGIST
FPO NEW YORK 09501-6002

COMSIXTHFLT/COMFAIRMED
ATTN: NSAP SCIENCE ADVISOR
FPO NEW YORK 09501-6002

COMMANDER NAVAL AIR FORCE
U.S. ATLANTIC FLEET
ATTN: NSAP SCIENCE ADVISOR
NORFOLK, VA 23511-5188

COMNAVAIRPAC
ATTN: NSAP SCIENCE ADVISOR
NAS, NORTH ISLAND
SAN DIEGO, CA 92135-5100

COMNAVSURFLANT
ATTN: NSAP SCIENCE ADVISOR
NORFOLK, VA 23511

COMNAVSURFPAC
(005/N6N)
ATTN: NSAP SCIENCE ADVISOR
SAN DIEGO, CA 92155-5035

COMSUBFORLANT
ATTN: NSAP SCI. ADV. (013)
NORFOLK, VA 23511

COMMANDER
AMPHIBIOUS GROUP 2
ATTN: METEOROLOGICAL OFFICER
FPO NEW YORK 09501-6007

COMMANDER
AMPHIBIOUS GROUP 1
ATTN: METEOROLOGICAL OFFICER
FPO SAN FRANCISCO 96601-6006

COMMANDER
OPTEVFOR
ATTN: NSAP SCIENCE ADVISOR
NORFOLK, VA 23511-6388

COMMANDER
CRUISER-DESTROYER GROUP 8
ATTN: STAFF OCEANOGR. (N35)
FPO NEW YORK 09501-4704

COMMANDING OFFICER
USS AMERICA (CV-66)
ATTN: MET. OFFICER, OA DIV.
FPO NEW YORK 09531-2790

COMMANDING OFFICER
USS CORAL SEA (CV-43)
ATTN: MET. OFFICER, OA DIV.
FPO NEW YORK 09550-2720

COMMANDING OFFICER
USS D. D. EISENHOWER (CVN-69)
ATTN: MET. OFFICER, OA DIV.
FPO NEW YORK 09532-2830

COMMANDING OFFICER
USS FORRESTAL (CV-59)
ATTN: MET. OFFICER, OA DIV.
FPO MIAMI 34080-2730

COMMANDING OFFICER
USS INDEPENDENCE (CV-62)
ATTN: MET. OFFICER, OA DIV.
FPO NEW YORK 09537-2760

COMMANDING OFFICER
USS J. F. KENNEDY (CV-67)
ATTN: MET. OFFICER, OA DIV.
FPO NEW YORK 09538-2800

COMMANDING OFFICER
USS NIMITZ (CVN-68)
ATTN: MET. OFFICER, OA DIV.
FPO NEW YORK 09542-2820

COMMANDING OFFICER
USS SARATOGA (CV-60)
ATTN: MET. OFFICER, OA DIV.
FPO MIAMI 34078-2740

COMMANDING OFFICER
USS T. ROOSEVELT (CVN-71)
ATTN: METEOROLOGY OFFICER
FPO NEW YORK 09559-2871

COMMANDING OFFICER
USS CONSTELLATION (CV-64)
ATTN: MET. OFFICER, OA DIV.
FPO SAN FRANCISCO 96635-2780

COMMANDING OFFICER
USS ENTERPRISE (CVN-65)
ATTN: MET. OFFICER, OA DIV.
FPO SAN FRANCISCO 96636-2810

COMMANDING OFFICER
USS KITTY HAWK (CV-63)
ATTN: MET. OFFICER, OA DIV.
FPO SAN FRANCISCO 96634-2770

COMMANDING OFFICER
USS MIDWAY (CV-41)
ATTN: MET. OFFICER, OA DIV.
FPO SAN FRANCISCO 96631-2710

COMMANDING OFFICER
USS RANGER (CV-61)
ATTN: MET. OFFICER, OA DIV.
FPO SAN FRANCISCO 96633-2750

COMMANDING OFFICER
USS CARL VINSON (CVN-70)
ATTN: MET. OFFICER, OA DIV.
FPO SAN FRANCISCO 96629-2840

COMMANDING OFFICER
USS IOWA (BB-61)
ATTN: MET. OFFICER, OA DIV.
FPO NEW YORK 09546-1100

COMMANDING OFFICER
USS NEW JERSEY (BB-62)
ATTN: MET. OFFICER, OA DIV.
FPO SAN FRANCISCO 96688-1110

COMMANDING OFFICER
USS MOUNT WHITNEY (LCC-20)
ATTN: MET. OFFICER
FPO NEW YORK 09517-3310

COMMANDING OFFICER
USS BLUERIDGE (LCC-19)
ATTN: MET. OFFICER
FPO SAN FRANCISCO 96628-3300

COMMANDING OFFICER
USS GUADALCANAL (LPH-7)
ATTN: MET. OFFICER
FPO NEW YORK 09562-1635

COMMANDING OFFICER
USS GUAM (LPH-9)
ATTN: MET. OFFICER
FPO NEW YORK 09563-1640

COMMANDING OFFICER
USS INCHON (LPH-12)
ATTN: MET. OFFICER
FPO NEW YORK 09529-1655

COMMANDING OFFICER
USS IWO JIMA (LPH-2)
ATTN: MET. OFFICER
FPO NEW YORK 09561-1625

COMMANDING OFFICER
USS NASSAU (LHA-4)
ATTN: MET. OFFICER
FPO NEW YORK 09557-1615

COMMANDING OFFICER
USS SAIPAN (LHA-2)
ATTN: MET. OFFICER
FPO NEW YORK 09549-1605

COMMANDING OFFICER
USS BELLEAU WOOD (LHA-3)
ATTN: METEOROLOGICAL OFFICER
FPO SAN FRANCISCO 96623-1610

COMMANDING OFFICER
USS NEW ORLEANS (LPH-11)
ATTN: MET. OFFICER
FPO SAN FRANCISCO 96627-1650

COMMANDING OFFICER
USS OKINAWA (LPH-3)
ATTN: MET. OFFICER
FPO SAN FRANCISCO 96625-1630

COMMANDING OFFICER
USS PELELIU (LHA-5)
ATTN: MET. OFFICER
FPO SAN FRANCISCO 96624-1620

COMMANDING OFFICER
USS TARAWA (LHA-1)
ATTN: MET. OFFICER
FPO SAN FRANCISCO 96622-1600

COMMANDING OFFICER
USS TRIPOLI (LPH-10)
ATTN: METEOROLOGICAL OFFICER
FPO SAN FRANCISCO 96626-1645

COMMANDING OFFICER
USS PUGET SOUND (AD-38)
ATTN: METEOROLOGICAL OFFICER
FPO NEW YORK 09544-2520

COMMANDING OFFICER
USS LASALLE (AGF-3)
ATTN: METEOROLOGICAL OFFICER
FPO NEW YORK 09577-3320

COMFLTAIR, MEDITERRANEAN
ATTN: NSAP SCIENCE ADVISOR
CODE 03A
FPO NEW YORK 09521

COMMANDING GENERAL
MARINE AMPHIBIOUS FORCE FMF
ATTN: NSAP SCI. ADV.
CAMP PENDLETON, CA 92055

COMMANDING GENERAL (G4)
FLEET MARINE FORCE, ATLANTIC
ATTN: NSAP SCIENCE ADVISOR
NORFOLK, VA 23511

USCINCPAC
BOX 13
STAFF CINCPAC J37
CAMP SMITH, HI 96861

USCINCENT
ATTN: WEATHER DIV. (CCJ3-W)
MACDILL AFB, FL 33608-7001

COMMANDER
US NAVAL FORCES CENTRAL COM.
PEARL HARBOR, HI 96860

ASST. FOR ENV. SCIENCES
ASST. SEC. OF THE NAVY (R&D)
ROOM 5E731, THE PENTAGON
WASHINGTON, DC 20350

CHIEF OF NAVAL RESEARCH (2)
LIBRARY SERVICES, CODE 784
BALLSTON TOWER #1
800 QUINCY ST.
ARLINGTON, VA 22217-5000

OFFICE OF NAVAL RESEARCH
CODE 1122AT, ATMOS. SCIENCES
ARLINGTON, VA 22217-5000

OFFICE OF NAVAL RESEARCH
ATTN: HEAD, OCEAN SCIENCES DIV
CODE 1122
ARLINGTON, VA 22217-5000

OFFICE OF NAVAL TECHNOLOGY
ONR (CODE 22)
800 N. QUINCY ST.
ARLINGTON, VA 22217-5000

CHIEF OF NAVAL OPERATIONS
(OP-006)
U.S. NAVAL OBSERVATORY
WASHINGTON, DC 20390

CHIEF, ENV. SVCS. DIV.
OJCS (J-33)
RM. 2877K, THE PENTAGON
WASHINGTON, DC 20301

NAVAL DEPUTY TO THE
ADMINISTRATOR, NOAA
ROOM 200, PAGE BLDG. #1
3300 WHITEHAVEN ST. NW
WASHINGTON, DC 20235

OFFICER IN CHARGE
NAVOCEANCOMDET
NAVAL STATION
FPO SEATTLE 98791-2943

OFFICER IN CHARGE
NAVOCEANCOMDET
BOX 81, USNAS
FPO SAN FRANCISCO 96637-2900

OFFICER IN CHARGE
NAVOCEANCOMDET
FEDERAL BLDG.
ASHEVILLE, NC 28801-2696

OFFICER IN CHARGE
NAVOCEANCOMDET
U.S. NAVAL AIR FACILITY
FPO SEATTLE 98767-2903

OFFICER IN CHARGE
NAVOCEANCOMDET
NAVAL AIR STATION
BARBERS PT., HI 96862-5750

CPOIC
NAVOCEANCOMDET
CHASE FIELD
BEEVILLE, TX 78103-5007

OFFICER IN CHARGE
NAVOCEANCOMDET
CARSWELL AFB, TX 76127

OFFICER IN CHARGE
NAVOCEANCOMDET
NAVAL AIR STATION
CECIL FIELD, FL 32215-0154

OFFICER IN CHARGE
NAVOCEANCOMDET
NAVAL STATION
CHARLESTON, SC 29408-6475

CPOIC
NAVOCEANCOMDET
NAVAL AIR FACILITY
CHINA LAKE, CA 93557-6001

OFFICER IN CHARGE
NAVOCEANCOMDET
NAVAL AIR STATION
CORPUS CHRISTI, TX 78419-5216

CPOIC
NAVOCEANCOMDET
NAVAL AIR STATION
DALLAS, TX 75211-9518

OFFICER IN CHARGE
NAVOCEANCOMDET
NAVAL AIR STATION
FALLON, NV 89406

OFFICER IN CHARGE
U.S. NAVOCEANCOMDET
BOX 16
FPO NEW YORK 09593-5000

OFFICER IN CHARGE
NAVOCEANCOMDET
NAS, BOX 9048
KEY WEST, FL 33040-5000

CPOIC
NAVOCEANCOMDET
NAVAL AIR STATION
KINGSVILLE, TX 78363-5130

OFFICER IN CHARGE
NAVOCEANCOMDET
NAVAL AIR STATION
LEMOORE, CA 93246-6001

OFFICER IN CHARGE
NAVOCEANCOMDET
NAVAL EDUCATION & TRNG CENTER
NEWPORT, RI 02841-5000

OFFICER IN CHARGE
NAVOCEANCOMDET, BOX 224
NAVAL AIR FACILITY
MAYPORT, FL 32228-0224

OFFICER IN CHARGE
NAVOCEANCOMDET
NAS, MEMPHIS
MILLINGTON, TN 38054-5220

OFFICER IN CHARGE
NNAVOCEANCOMDET
NAS, WHITING FIELD
MILTON, FL 32570-5160

OFFICER IN CHARGE
NAVOCEANCOMDET
NAVAL AIR STATION
MERIDIAN, MS 39309-0033

OFFICER IN CHARGE
NAVOCEANCOMDET
MONTEREY, CA 93943-5004

OFFICER IN CHARGE
U.S. NAVOCEANCOMDET
APO SAN FRANCISCO 96519-5000

OFFICER IN CHARGE
NAVOCEANCOMDET
NAVAL AIR STATION
MOFFETT FIELD, CA 94035

OFFICER IN CHARGE
U.S. NAVOCEANCOMDET
NAPLES, BOX 23
FPO NEW YORK 09520-0800

CPOIC
NAVOCEANCOMDET
NAVAL AIR STATION
NEW ORLEANS, LA 70143-1300

OFFICER IN CHARGE
NAVOCEANCOMDET
NAS, WHIDBEY ISLAND
OAK HARBOR, WA 98278-5100

OFFICER IN CHARGE
NAVOCEANCOMDET
AFGWC
OFFUTT AFB, NE 68113

OFFICER IN CHARGE
NAVOCEANCOMDET
NAVAL AIR STATION
PATUXENT RIVER, MD 20670-5103

OFFICER IN CHARGE
NAVOCEANCOMDET
U.S. NAVAL STATION
FPO MIAMI 34051-9300

OFFICER IN CHARGE
NAVOCEANCOMDET
NAVAL AIR STATION
SAN DIEGO, CA 92145-5851

OFFICER IN CHARGE
NAVOCEANCOMDET
U.S. NAVAL AIR FACILITY
FPO NEW YORK 09523-2900

OFFICER IN CHARGE
U.S. NAVOCEANCOMDET
FPO NEW YORK 09528-0109

OFFICER IN CHARGE
NAVOCEANCOMDET
NAVAL AIR STATION
SOUTH WEYMOUTH, MA 02190-5005

OFFICER IN CHARGE
NAVOCEANCOMDET
NAS, OCEANA
VIRGINIA BEACH, VA 23460-5120

OFFICER IN CHARGE
NAVOCEANCOMDET
NAVAL AIR STATION
WILLOW GROVE, PA 19090-5010

OFFICER IN CHARGE
U.S. NAVOCEANCOMDET
FPO SAN FRANCISCO 96635-2905

OFFICER IN CHARGE
U.S. NAVOCEANCOMDET
FLEET ACTIVITIES
FPO SEATTLE 98770-0051

OFFICER IN CHARGE
NAVOCEANCOMDET
NAVAL AIR STATION
ALAMEDA, CA 94501-5011

OFFICER IN CHARGE
NAVOCEANCOMDET
NAVAL AIR STATION
PENSACOLA, FL 32508-7200

CPOIC
NAVOCEANCOMDET
NAVAL AIR STATION
GLENVIEW, IL 60026-5170

OFFICER IN CHARGE
U.S. NAVOCEANCOMDET
APO NEW YORK 09406-5000

OFFICER IN CHARGE
NAVOCEANCOMDET
NAVAL AIR STATION
LONG BEACH, CA 90822-5072

COMMANDING OFFICER
NAVAL RESEARCH LAB
ATTN: LIBRARY, CODE 2620
WASHINGTON, DC 20390

OFFICE OF NAVAL RESEARCH
SCRIPPS INSTITUTION OF
OCEANOGRAPHY
LA JOLLA, CA 92037

COMMANDING OFFICER
NAVAL OCEAN RSCH & DEV ACT
NSTL, MS 39529-5004

COMMANDER
NAVAL OCEANOGRAPHY COMMAND
NSTL, MS 39529-5000

COMMANDING OFFICER
FLENUMOCEANCEN
MONTEREY, CA 93943-5005

COMMANDING OFFICER
NAVWESTOCEANCEN
BOX 113
PEARL HARBOR, HI 96860

COMMANDING OFFICER
NAVEASTOCEANCEN
MCADIE BLDG. (U-117), NAS
NORFOLK, VA 23511-5399

COMMANDING OFFICER
NAVPOLAROCEN, NAVY DEPT.
4301 SUITLAND RD
WASHINGTON, DC 20395-5180

COMMANDING OFFICER
U.S. NAVOCEANCOMCEN
BOX 12, COMNAV Marianas
FPO SAN FRANCISCO 96630-2926

COMMANDING OFFICER
U.S. NAVOCEANCOMCEN
BOX 31 (ROTA)
FPO NEW YORK 09540-3200

COMMANDING OFFICER
NAVOCEANCOMFAC
P.O. BOX 85, NAS
JACKSONVILLE, FL 32212-0085

COMMANDING OFFICER
NAVOCEANCOMFAC
NAS, NORTH ISLAND
SAN DIEGO, CA 92135

COMMANDING OFFICER
U.S. NAVOCEANCOMFAC
FPO SEATTLE 98762-3500

COMMANDING OFFICER
NAVOCEANCOMFAC
NSTL, MS 39529-5002

COMMANDING OFFICER
U.S. NAVOCEANCOMFAC
FPO NEW YORK 09571-0926

COMMANDING OFFICER
U.S. NAVOCEANCOMFAC
BOX 63, NAS (CUBI PT)
FPO SAN FRANCISCO 96654-2909

COMMANDING OFFICER
U.S. NAVOCEANCOMFAC
NAVAL AIR STATION
FPO NEW YORK 09560-5025

COMMANDING OFFICER
NAVOCEANCOMFAC
NAVAL AIR STATION
BRUNSWICK, ME 04011-5000

SUPERINTENDENT
LIBRARY REPORTS
U.S. NAVAL ACADEMY
ANNAPOLIS, MD 21402

CHAIRMAN
OCEANOGRAPHY DEPT.
U.S. NAVAL ACADEMY
ANNAPOLIS, MD 21402

NAVAL POSTGRADUATE SCHOOL
METEOROLOGY DEPT.
MONTEREY, CA 93943-5000

NAVAL POSTGRADUATE SCHOOL
PHYSICS & CHEMISTRY DEPT.
MONTEREY, CA 93943-5000

LIBRARY
NAVAL POSTGRADUATE SCHOOL
MONTEREY, CA 93943-5002

PRESIDENT
NAVAL WAR COLLEGE
GEOPHYS. OFFICER, NAVOPS DEPT.
NEWPORT, RI 02841

COMMANDER
NAVAL SAFETY CENTER
NAVAL AIR STATION
NORFOLK, VA 23511

COMMANDER
NAVAIRSYSCOM, CODE 526W
WASHINGTON, DC 20361-0001

COMSPAWARSYSCOM
ATTN: CAPT. R. PLANTE
CODE 3213, NAVY DEPT.
WASHINGTON, DC 20363-5100

COMSPAWARSYSCOM
ATTN: CODE PMW 145, NAVY DEPT.
WASHINGTON, DC 20363-5100

COMMANDER
NAVOCEANSYSCEN
DR. J. RICHTER, CODE 54
SAN DIEGO, CA 92152-5000

COMMANDER
PACMISTESTCEN
GEOPHYSICS OFFICER
PT. MUGU, CA 93042

USAFETAC/TS
SCOTT AFB, IL 62225

DIRECTOR (10)
DEFENSE TECH. INFORMATION
CENTER, CAMERON STATION
ALEXANDRIA, VA 22314

DIRECTOR, ENV. & LIFE SCI.
OFFICE OF UNDERSECRETARY OF
DEFENSE FOR RSCH & ENG E&LS
RM. 3D129, THE PENTAGON
WASHINGTON, DC 20505

FEDERAL COORD. FOR METEORO.
SERVS. & SUP. RSCH. (OFCM)
11426 ROCKVILLE PIKE
SUITE 300
ROCKVILLE, MD 20852

DIRECTOR
NATIONAL SEVERE STORMS LAB
1313 HALLEY CIRCLE
NORMAN, OK 73069

JOHNS HOPKINS UNIVERSITY
ATTN: JIM SCHNEIDER
APPLIED PHYSICS LAB
JOHNS HOPKINS RD.
LAUREL, MD 20707

WAVE PROPAGATION LAB
NOAA
325 S. BROADWAY
BOULDER, CO 80303

NAVSEASYSKOM
MR. D. BRITTON, PMS-400B3B
RM 10N08 NC2
WASHINGTON, DC 30362

COL. RAMSEY JOHNSON
COMMANDER, AFGL
HANSKOM AFB, MA 01731

SCRIPPS INSTITUTION OF
OCEANOGRAPHY
ATTN: J. SIMPSON
LA JOLLA, CA 92037

PENNSYLVANIA STATE UNIVERSITY
ATTN: G. FARRELL, METEOROLOGY
DEPARTMENT
503 DEIKE BLDG.
UNIVERSITY PARK, PA 16802

THE EXECUTIVE DIRECTOR
AMERICAN METEORO. SOCIETY
45 BEACON ST.
BOSTON, MA 02108

AMERICAN METEORO. SOCIETY
METEOR. & GEOASTRO. ABSTRACTS
P.O. BOX 1736
WASHINGTON, DC 20013

DUDLEY KNOX LIBRARY - RESEARCH REPORTS



5 6853 01078592 6

U230929